Geophysical and social vulnerability to floods at municipal scale under climate change: The case of an inner-city suburb of Sydney

Ecological Indicators 121 (2021) 106988

Contents lists available at ScienceDirect

Ecological Indicators

journal homepage: www.elsevier.com/locate/ecolind

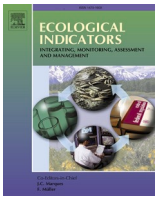

Geophysical and social vulnerability to floods at municipal scale under climate change: The case of an inner-city suburb of Sydney

Abbas El-Zein [a,*], Tanvir Ahmed [b], Fahim Tonmoy [c,d]

[a] School of Civil Engineering, University of Sydney, NSW 2006, Australia
[b] Shoalhaven City Council, Nowra, NSW 2541, Australia
[c] BMT Commercial Australia Pty Ltd, 200 Creek Street, Brisbane, QLD 4000, Australia
[d] School of Engineering and Built Environment, Griffith University, QLD 4222, Australia

ARTICLE INFO

Keywords:
Flood
Vulnerability
Social vulnerability
Climate change
Sea level rise
Municipal planning

ABSTRACT

Assessments of vulnerability to flooding can generate useful data for planners and policy makers. To the best of the authors knowledge, no flood-vulnerability study has combined geophysical modelling of floods with socio-economic assessments of vulnerability at finer municipal or household scale. In addition, the extent to which vulnerability assessments actually feed into flood adaptation policies remains largely unknown.

A new flood vulnerability index, and associated methodology, is proposed, combining high-resolution hydrological-hydraulic modelling with built-environment and socio-economic indicators at the smallest spatial scale at which socio-economic data is available. The main advantage of the methodology is its ability to incorporate place-specific data, hence yielding more refined simulations of floods and the capacity to make projections into climate futures at local scale. The index is built and applied to the inter-city suburb of Marrickville in Sydney and used to assess the effects of future climate change on vulnerability mapping in the suburb. Finally, the results of the assessment are presented to, and discussed with, the local government authority responsible for implementing flood adaptation policies for Marrickville.

Locally specific modelling of floods, combined with socio-economic and built-environment mapping, has yielded a rich set of information on flood vulnerability and significant variability within a single suburb. Flood duration is projected to increase by more than 100% under some climate change scenarios, as a result of reduced drainage caused by sea level rise. Feedback from municipal council has highlighted the potential usefulness of the knowledge generated by the assessment, especially for emergency services.

1. Introduction

Climate change is expected to increase weather-related hazards including floods (Jongman, 2015). Considering only projected population growth, urbanization and growth in economic activity, but without accounting for increases in flood frequency and intensity, the average annual global flood losses are set to increase by a factor of nine from 2005 to 2050. If the effects of climate change are included, losses increase by a factor of more than 17 (Hallegatte et al., 2013).

In recent years, a body of literature has enhanced our understanding of the physical behavior of floods, including predictions of future flooding scenarios (Zhou et al., 2016; Domingo et al., 2010; Patro et al., 2009; Sole et al., 2008; Overton, 2005; Hallegatte et al., 2013). In addition, several studies have proposed and/or analysed flood management strategies aimed at reducing economic damage and assisting communities in adapting to flooding events (Muis et al., 2015; Tavares et al., 2015; Garbutt et al., 2015; Hunt and Watkiss, 2011).

Flood assessments in the peer-reviewed and grey literature have typically focused on the geophysical and geomorphological determinants of floods (Mucerino, et al., 2018), deriving depth-damage relationships, usually based on physical damage to property, or developing estimates of frequency and areal extent of flooding (Reid et al., 2014; Shakrabarty, 2017; Rehan, 2018). These studies often make recommendations for improving drainage paths and upgrading storm water infrastructure. On the other hand, several authors have shown that social vulnerabilities may limit access by individuals and communities to resources during floods, hence increasing their susceptibility to flood impacts and reducing their capacity to cope and/or recover. They

* Corresponding author.
E-mail address: abbas.elzein@sydney.edu.au (A. El-Zein).

https://doi.org/10.1016/j.ecolind.2020.106988
Received 2 March 2020; Received in revised form 15 June 2020; Accepted 18 September 2020
Available online 13 October 2020

argued for an approach to flood management that goes beyond geophysical assessments of vulnerability and economic valuations of its impacts, to include factors such as social disadvantage, built environment and institutional capacity, amongst others (Tapsell et al., 2002; Kammerbauer and Wamsler, 2018). This was emphasised by the International Panel on Climate Change (IPCC), starting from its third assessment report, which proposed a concept of vulnerability that includes three components or dimensions, namely exposure, sensitivity and coping capacity.

Flood vulnerability mapping has been conducted at city- or town-scale (Connor and Hiroki, 2005; Balica and Wright, 2012; Yang et al., 2018; Szewrański et al., 2018; Lee and Il Choi, 2018), municipal scale (Fernandez et al., 2016; Zachos et al., 2016) or a finer household level (Brouwer et al., 2007; Bhattacharjee and Behera, 2018; Rana and Routray, 2018; Solín, 2017). Studies conducted at larger scales can generate valuable data at the upstream end of a top-down planning process, helping authorities to identify priority regions and actions. However, given its usually poor spatial resolution, it has limited use for local councils hoping to develop place-specific flood mitigation policies. Municipalities require local data and strategies that can identify populations and assets at risk, and help develop specific measures to reduce vulnerability and increase resilience (Queste et al., 2013; Török, 2018). Such measures are often inscribed within, and informed by, larger-scale policies but are not entirely determined by them.

Several flood-assessment studies, incorporating social vulnerability, have been conducted at a finer-scale resolution. Koks et al. (2015) built a flood vulnerability index for the city of Rotterdam in the Netherlands, based on flood-hazard zones, exposed assets and spatially detailed demographic and socio-economic data from the Census. They highlighted the heterogeneity of the population and the multiple sources of vulnerability to flooding. Both Fernandez et al. (2016) and Zachos et al. (2016) developed flood vulnerability indices based on social, economic, environmental and built-environment indicators. The former applied the index to a municipality in Portugal while the latter used it to study flooding in the lower Mississippi. Török (2018) assessed vulnerability to flooding at the lowest administrative scale in Romania, incorporating demographic structure, the built environment and socio-economic status as three sets of indicators reflecting vulnerability. None of the four, above-mentioned studies have incorporated their own place-specific simulations of flooding in the assessment.

To the best of the author's knowledge, no composite index of vulnerability to flooding, incorporating both geophysical and socio-economic dimensions of risk and using hydrologic simulations of floods, was developed at a local municipal scale. One of the advantages of incorporating hydraulic modelling of floods in indicator-based vulnerability assessments is that the tool thus developed can be used to study the effects of climate change (e.g., changes in rainfall patterns; rise in sea level) on vulnerability. Furthermore, an underlying assumption is found in the body of literature discussed above that vulnerability assessments are useful for the development of adaptation action and policy. However, there is very little evidence of this. In fact, the extent to which vulnerability assessments actually feed into flood adaptation policies remains largely unknown (Ford et al., 2018).

The goal of this paper is threefold. A new flood vulnerability index is proposed, combining high-resolution hydrological-hydraulic modelling of floods with built environment and socio-economic indicators at the smallest spatial scale for which socio-economic data is available. The new index is built and applied to the inter-city suburb of Marrickville in Sydney. The value of overlaying detailed geophysical and socio-economic flood data at local scale is hence evaluated. Next, the new index is used to assess the effects of future climate change on vulnerability mapping in the municipality. Finally, the results of the assessment are presented to the local government council responsible for implementing flood adaptation policies for Marrickville. Hence, the reception of the vulnerability assessment by a policy-development agency is evaluated.

The remainder of the paper is structured as follows. First, the concept of vulnerability to flooding is defined, the literature on social vulnerability is reviewed and challenges posed by flood vulnerability assessments are discussed. Second, key characteristics of the study area are described, and the methodologies followed in this study are presented – including flood modelling, indicator selection for built-environment and social vulnerabilities, and climate change scenarios. Results of analyses are then presented, including the outcomes of the focus group at the Marrickville council, followed by a discussion of the implications of our findings.

2. Vulnerability to flooding

2.1. Vulnerability concept

Vulnerability can be defined as the degree to which a socio-ecological system is likely to experience harm due to exposure to a hazard (Turner, et al., 2003). While this definition appears to be widely accepted, how to operationalise it with a view of quantifying vulnerability remains an open question. To start with, the words "harm", "exposure" and "hazard" are each open to wide interpretation, and the relationships between them equally so. In addition, the task is made more challenging by the multidisciplinary content of the literature on vulnerability since the concept has been employed in geography, economics, sociology, disaster management, environmental science and health.

Rygel et al. (2006) points to two major perspectives in vulnerability research. The first approach focuses on the potential exposure to hazards. Studies conducted by following this theme, aim to assess the impact of hazards and the degree of loss of life and property resulting from a particular event (Muis et al., 2015; Van Manen and Brinkhuis, 2005; Tapsell et al., 2002). The second major perspective highlights differential impacts from hazards and attempts to explain why two different communities exposed to the same magnitude of hazard may experience its impacts in different ways and to different extents (Cutter et al., 2013; Sarewitz et al., 2003). This is referred to as social vulnerability which is defined by Sarewitz et al. (2003) as those intrinsic characteristics of individuals, households and communities that increase their potential to be harmed.

Empirical evidence from historical flood analysis has indeed shown that particular social groups tend to carry a higher burden of death, injury and economic impact from floods (Solangaarachchi et al., 2012). For example, populations with low income and ethnically diverse mix in Texas, USA experienced a higher number of casualties from floods (Zahran et al., 2008). Individuals and communities with low incomes have higher dependence on welfare while low-skilled workers may lose their sources of income during or after the disaster, all of which may slow down and obstruct recovery from disasters (Cutter et al., 2003). Those who have pre-existing medical conditions, are physically impaired, physically dependent, live alone in a household, or are a primary carer in a single-parent household with dependent children, may require extra attention in times of hazard and may sometimes be overlooked during the recovery phase due to their low visibility (O'Brien and Mileti, 1993; Cutter et al., 2000; Blaikie et al., 2014). Women may be disadvantaged during recovery from a natural hazard because of lower earnings and extra family care responsibilities and household tasks (Cutter et al., 2003; Fekete, 2009). Individuals with higher education levels may be better able to access, interpret and act upon information and evacuation plans in times of disaster (Morrow, 1999; Solangaarachchi et al., 2012). Race, ethnicity and migration status are also important factors that may partly determine vulnerability to a hazard (Watts et al., 2009). For example, Pulido (Pulido, 2000) has shown how racial spatialization in Los Angeles has led Latinos and African-American communities to occupy environmentally marginal land with higher exposure to hazards. Poor familiarity of new migrants with place of residence, language barriers as well as lack of social

network, could make it harder for them to access emergency services. Other factors contributing to vulnerability include lack of access to motorised transport and to the internet (Watts et al., 2009).

All in all, the socio-economic, demographic and racial factors discussed above make it harder for communities to cope with, adapt to and recover from disasters (Cutter et al., 2013). In addition, aspects of the built environment such as high settlement density, poor quality of infrastructure, poor availability of medical facilities, that may or may not be correlated to socio-economic factors, can lead to worse impacts from natural hazards (Borden et al., 2007; Holand et al., 2011). An obvious example relevant to flooding is poor drainage infrastructure.

2.2. Assessment of social vulnerability

Indicator-based assessments of social vulnerability are widely used in the literature owing to the relative ease with which such indicators can be built or accessed. Assessments have been conducted at household (Dwyer et al., 2004), municipal (Solangaarachchi et al., 2012; Koks et al., 2015; Tavares et al., 2015; Apotsos, 2019), district (Holand et al., 2011; Garbutt et al., 2015; Kirby et al., 2019), regional (Cutter et al., 2003) and national (Vincent, 2004) scales[1]. The choice of spatial scale and geographical extent depends on the purpose of the study and the availability of information, usually taken from census data. The main advantage of finer scales is that they produce a richer set of information albeit at the cost of more intensive data gathering and analysis efforts. On the other hand, smaller geographical extent allows place-specific information and indicator selection to be made, but have relevance, by and large, only to the area under study.

The most common types of social vulnerability indicators used in the above-mentioned studies are i) dependency on others due to age or disability, ii) gender iii) economic disadvantage iv) occupation category v) limited access to resources including technology and transportation v) quality of accommodation vi) immigration status vii) language barriers and vii) race and ethnicity (Cutter et al., 2003, 2013; Borden et al., 2007; Schmidtlein et al., 2008; Fekete, 2009; Holand et al., 2011; Solangaarachchi et al., 2012; Garbutt et al., 2015; Koks et al., 2015; Tavares et al., 2015; Frigerio and De Amicis, 2016; Fatemi et al., 2016). Indicators are sometimes aggregated into an index such as the Social Vulnerability Index SoVI (Cutter et al., 2003).

Selecting the right indicators and the right aggregation approaches is far from trivial (Holand et al., 2011; Tonmoy et al., 2014; El-Zein and Tonmoy, 2017). Vulnerability is usually conceived of as constant in time and yet communities may move in and out of vulnerability which requires a more dynamic framing of the concept. Indicators acting as proxies for vulnerability may have different significance at different stages of a disaster (Rufat et al., 2015). For example, a relatively high percentage of children in a community may render it vulnerable during the disaster but might play a positive role in recovery. At the data-analysis stage, some indicators used for constructing vulnerability indices may be correlated and researchers typically apply statistical techniques, such as the principal component analysis (PCA), to remove correlations by reducing the variables into a number of algebraically independent components which capture most of the variability (Fekete, 2009; Tavares et al., 2015).

Additive or multiplicative aggregation is commonly used in combining multiple vulnerability indicators into a single vulnerability index and the choice of aggregation method has generated some debate in the literature (Ebert and Welsch, 2004; El-Zein and Tonmoy, 2015, 2017). Another important question is whether equal or different weights should be applied with a majority of studies appears to have assigned equal weights, partly because of lack of viable alternatives (Cutter et al., 2003; Schmidtlein et al., 2008; Solangaarachchi et al., 2012; Tavares et al., 2015). For an extensive discussion of this question the reader is referred to references (Tonmoy et al., 2014; El-Zein and Tonmoy, 2015, 2017).

3. Methodology

3.1. Conceptual framework

A widely used conceptual framework of vulnerability represents the impacts of floods as the outcome of interactions between the three dimensions of hazard, exposure and social vulnerability (Crichton, 2002; Dwyer et al., 2004; Lindley et al., 2006; Dang et al., 2011; Kaźmierczak and Cavan, 2011). The framework has been depicted as a pyramid whereby an increase in any one of the three dimensions increases the volume of the pyramid, reflecting higher vulnerability (Dwyer et al., 2004).

The "hazard" dimension is traditionally used in risk assessments and characterized by the probability of occurrence of the hazard in question (Dwyer et al., 2004). However, when outcomes of detailed flood simulations are available for different climate change scenarios, the areal extent, depth and duration of flooding as well as the water velocity during flood events, can be taken as "hazard" indicators instead (Plate, 2002; Schanze et al., 2006). In our methodology, these four variables are extracted from detailed hydrological-hydraulic modelling and combined into a flood hazard index.

"Exposure" is the extent to which valued aspects of a community's life (e.g., health, prosperity, security) are likely to be affected by the hazard in question (Dwyer et al., 2004; Koks et al., 2015). In the case of floods, a key mediator of impacts is the quality of the built environment, including population density, quality of building stock and quality of water drainage infrastructure. In this paper, water drainage infrastructure is incorporated by the spatially detailed hydrological-hydraulic simulations and will hence by reflected in the "hazard" rather than the "exposure" dimension. Therefore, "exposure" was characterised based on the demographic density and quality of the building stock only. Finally, for "social vulnerability", we followed the work of Cutter et al. (Cutter et al., 2003) and built a social vulnerability index using data obtained from the Australian Bureau of Statistics (ABS) as will be detailed later.

3.2. Study area

The Marrickville valley is an inner-city region of Sydney and part of the Inner West local government area (LGA) in the state of New South Wales (NSW) (see Fig. 1a and 1b). It has experienced significant flooding in the past, including as recently as 2012 (Mckenny, 2009). Its land use is medium-density residential housing (63%) and low-density, light industries, mainly automotive repair, building supplies and food processing (21%) (Fig. 1c). The remaining land use is parkland, commercial precincts, schools and roads. From the 2016 census data, Marrickville's total population was 26,592 with a median age of 36. 63.4% of the total population engaged in full-time employment with a median weekly household income of A$1,814 and median weekly rent of A$450. At census time, 29.4% of people were attending an educational institution, 16.2% of which were tertiary.

The topography of the area has been extracted from an Airborne Laser Survey (ALS), and found to vary from 5.5 to 50.8 mAHD (Fig. 1b). The Marrickville valley consists of 9 sub-catchments (see Fig. 1d) with the stormwater flowing south towards the Cooks River (Fig. 1e) via two sets of drainage systems. Property drainage systems (pipe/gutter) are linked with the pits/pipe systems whereupon water is conveyed to four major trunks, shown in Fig. 1f, before discharging to the Cooks River (Shakrabarty, 2017). The Marrickville Oval functions as a flood

[1] We take "spatial scale" to mean "spatial resolution", that is the smallest spatial unit ascribed an indicator value (e.g., household, street block, neighbourhood, district up to a whole nation), rather than the size of the total geographical area covered by the study; we refer to the latter as "geographical extent" of the study.

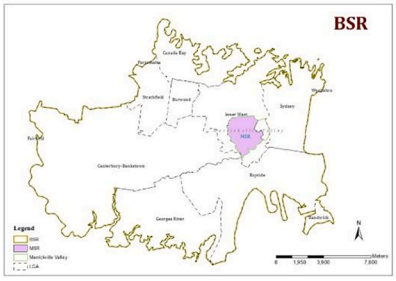

a. Marrickville Study Region (MSR) and Broader Study Region (BSR)

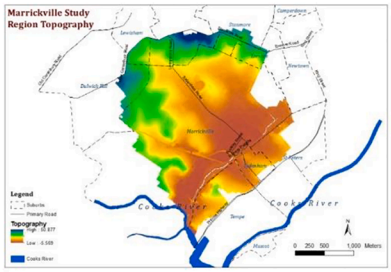

b. Topography of MSR

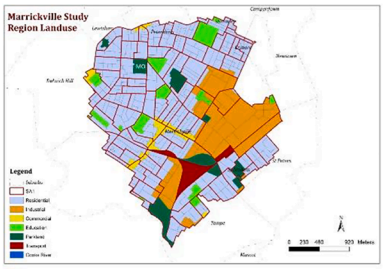

c. Land Use in MSR (location of Marrickville Oval indicated with MO)

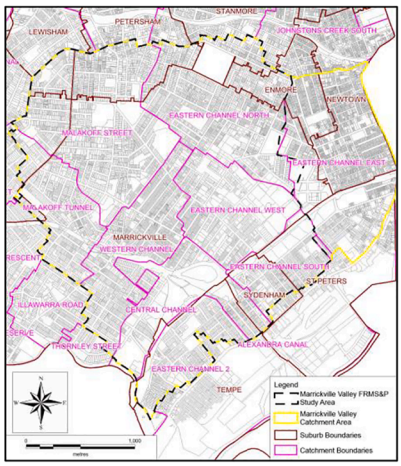

d. Sub-catchments in Marrickville Valley

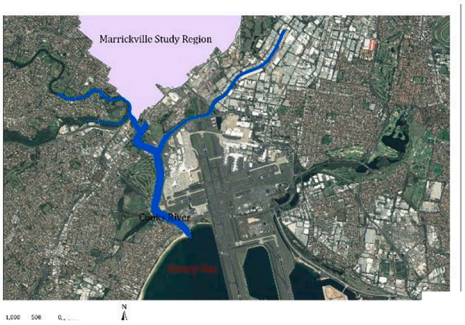

e. Confluence of the Cooks River

f. Drainage trunks

Fig. 1. Key characteristics of study area.

retarding basin (see Fig. 1c). The Sydenham storage pit serves the same purpose, but two pumps are installed in this pit to divert high flood water to the eastern channel. One pump is used to divert flood water to the Cooks River from the low lying area of the central channel catchment, and another one transfers water from the central channel to the eastern channel. Under flood conditions, drainage capacity is exceeded. Except under extreme flood events, overland flow towards the Cooks River is not possible due to urban barriers (Shakrabarty, 2017).

The specific region covered by the present study is referred to henceforth as the Marrickville Study Region (MSR) and was determined by the availability of data for flood modelling. It consisted of the Marrickville valley except for a small portion in the North-East. MSR includes 74% of the administrative Marrickville suburb, while 65% of MSR overlaps with it, with the rest coming from the suburbs of Tempe (8%), Petersham (7%), Dulwich Hill (5%), St Peters (4%), Sydenham (4%), Stanmore (3%), Enmore (2%) and Lewisham (2%).

3.3. Study scope

Following Tonmoy et al. (Tonmoy et al., 2014) and El-Zein & Tonmoy (El-Zein and Tonmoy, 2015), the scope of the vulnerability study was defined at the outset by providing answers to a set of questions, shown in table 1. The aim of the study was to assess the vulnerability of the well-being of Marrickville residents to flooding. Future projections of vulnerability were made for various climate change scenarios under *current* socio-economic and built-environment conditions. This was clearly an approximation of the future; however, attempting to project land use, demographic and socio-economic trends in Marrickville decades into the future would be highly challenging, riven with uncertainty and well beyond the scope of this study.

The smallest spatial unit of the study was determined by the

Table 1
Scope and Boundaries of Vulnerability Study.

Key Variable	Question	Definition
Geographical Scope	*Whose* vulnerability and over *what* geographical area?	Residents of Marrickville Study Region (MSR)
Valued Attribute	The vulnerability of *which valued attribute* of the socio-ecological system?	Well-being, including safety, health and economic prosperity, of MSR and BSR residents
Hazard	Vulnerability to *which hazard*?	Flooding as a result of extreme rainfall events (with or without climate change and sea level rise)
Dimensions of Vulnerability	*Which* dimensions of vulnerability are included?	Geophysical (hazard); Exposure (built environment); Socio-economic (social vulnerability)
Quantification	*How* will each dimension be quantified?	Geophysical: indicators extracted from fine-scale hydrological-hydraulic modelling; Built environment and socio-economic: indicators extracted from existing databases
Temporal Scale	Under *what scenarios* of climatic, institutional and socio-economic change?	Current social vulnerability and built environment + current and future climate (present, 2060 and 2080).
Spatial Scale	What is the basic *spatial unit* of the analyses?	Statistical Area Level 1 (SA1) (200–800 households per SA1; a total of 84 SA1s in the study area)

publically available socio-economic data from the ABS, namely the Statistical Area 1 (SA1). The whole of Australia is covered by a total of 54,805 SA1s and, typically, each SA1 contains between 200 and 800 capita with an average population of about 400. The areal extent of SA1 varies between regional and metropolitan zones. Note that hydrological modelling and data were initially generated at scales finer than SA1, then upscaled to SA1 level.

A structure of indicators was built based on the conceptual framework developed earlier. The structure, shown in Fig. 2a, was made of three indices corresponding to the three dimensions of risk: i) the flood hazard index (F_H), ii) the flood exposure index (F_E) and iii) the social vulnerability index (SoVI). The three indices were finally combined to build a Flood Social Vulnerability Index (FSVI) which provided a measure of relative vulnerability to flooding among different spatial units of the flood-prone region.

As Fig. 2b shows, the dataset for each indicator is first standardised relative to the mean and standard deviation and then the set of normalised indicators is aggregated additively to generate an index. Each index is rescaled to a value between 1 and 10 and then the three indices are combined, using summative or multiplicative aggregations, to produce FSVI. As discussed earlier, it is difficult to generate a rationale for unequal weights and therefore, after consultation with the Inner West

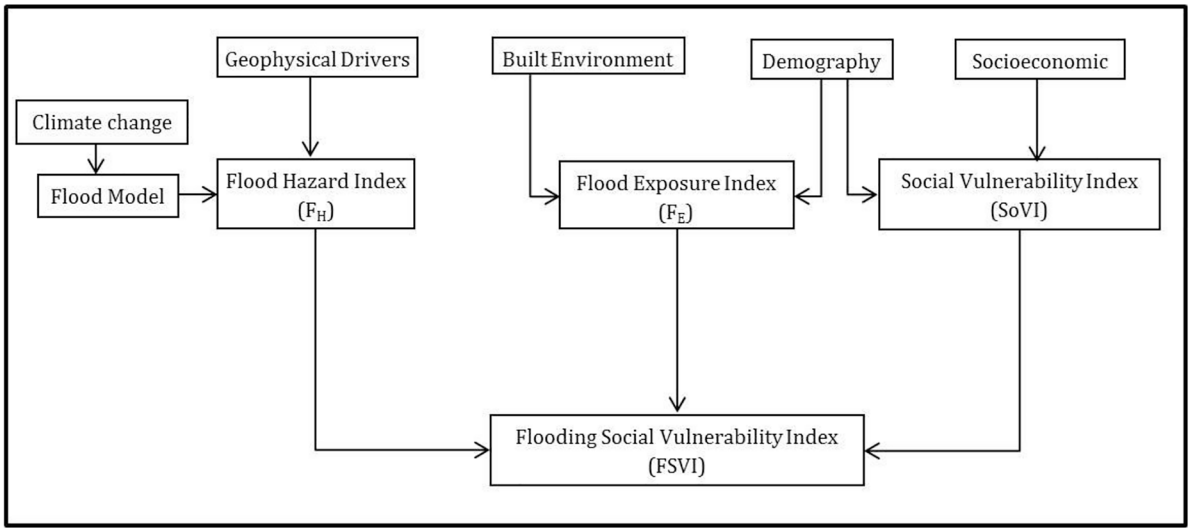

a) Flood Social Vulnerability Index overall structure

i. Study area subdivided into a number of spatial units preferably the smallest geographical unit for which demographic and socioeconomic data is available.

ii. Each vulnerability dimension is quantified as an index built upon a set of indicators. The indicators are selected to capture major elements of the dimension in question. The indicators are standardised with a mean of 0 and standard deviation of 1:

$$I_{si} = \frac{I_i - \mu_i}{\sigma_i} \quad (1)$$

where I_{si} is the standardised value of the indicator I_i, μ_i and σ_i are the mean and standard deviation of I_i set for all the spatial units within the study area. Each of the three indices is built by additive aggregation of indicators according to:

$$F_m = \sum_{i=1}^{N_m} w_i I_{si} \quad (2)$$

where F is the index of the dimension m (i.e., flood hazard, flood exposure or social vulnerability), I_{si} is the standardised value of the i^{th} indicator, w_i is the weight of indicator I_i and N_m is the number of indicators for dimension m.

iii. The index value of each of the three vulnerability dimensions is normalized and converted into a value between 1 and 10, where 1 indicates the lowest vulnerability and 10 the highest.

iv. Finally, the three indices are combined to calculate a Flood Social Vulnerability Index (FSVI), following additive or multiplicative aggregation:

Additive aggregation: $FSVI_{Ai} = w_h F_{Hi} + w_e F_{Ei} + w_s SoVI_i$ (3)

where, w_h, w_e and w_s are weight of the three indices

Multiplicative aggregation: $FSVI_{Mi} = {F_{Hi}}^{p_h} \times {F_{Ei}}^{p_e} \times {SoVI_i}^{p_s}$ (4)

where p_h, p_e and p_s are the multiplication weights of the three indices.

b) Step-by-step procedure for building index

Fig. 2. Flooding Social Vulnerability Index construction.

Council stakeholders, equal weights were used in this study. The methods used in developing/selecting indicators for F_H, F_E and SoVI are described next.

3.4. Flood modelling

In 2012, the local municipal authority responsible for the MSR (previously Marrickville Council now part of the Inner West Council) built a hydrological-hydraulic simulation, using software DRAINS and TUFLOW (described below) (O'Loughlin et al., 2018). The outcomes of the Council's simulations had not been combined with any socio-economic or built-environment assessment of vulnerability. The Council's models were used as starting points for our study to generate flooding simulations from extreme rainfall for a base case and climate change scenarios.

To build the base case, we updated the Council's 2012 flood models with new sets of temporal rainfall patterns, known as ensemble storms based on the Australian Rainfall-Runoff (ARR) 2016 Intensity Frequency Duration (IFD) curves/charts (Ball, 2016). These are probabilistic estimations of average rainfall depth at a particular location over a given duration, developed by the Australian Bureau of Meteorology (BOM). A 1% Annual Exceedance Probability (AEP) which fell into the category of Rare Design Rainfall and had a 1% chance of occurring in a given year was selected from the median of the storm ensemble as the design storm event (Ball, 2016). A total of 1035 hydrological sub-catchments were generated based on the Airborne Laser Survey (ALS) with the assumption that runoff discharged from those sub-catchments would flow towards pits.

To conduct the simulations, we first used the DRAINS code (hydrological modelling) to generate surface stream flows arriving at each pit. The DRAINS model solved the Mannings equation to convert rainfall from the design storm event into stormwater hydrographs of water arriving into the pits from each sub-catchment, after accounting for losses to ground infiltration. Next, we entered the hydrographs into TUFLOW (hydraulic modelling) in order to simulate flooding while accounting for topography, roads, levees, infrastructures, including the stormwater drainage systems. TUFLOW solved the unsteady depth-averaged momentum and continuity equations (i.e., Navier-Stokes equations) for free-surface flow. TUFLOW was also dynamically coupled with ESTRY, which solved the 1D free-surface St Venant flow equations and was hence suitable for modelling flow in narrow open channels, stormwater pipes, culverts, bridges, weirs, trunks and pumps. The TUFLOW simulations were conducted on a 3mx3m grid, which is a much finer spatial resolution than the SA1 scale of socio-economic data.

No historical gauge water level and discharge data were available for the study area and results of the original 2012 model were therefore verified based on the council knowledge of drainage hot spots, community questionnaire results and comparison of results with previous studies.

3.5. Climate change scenarios

Climate change scenarios were constructed as variations on the base case, as described next. Potential variations of flooding patterns in Marrickville due to future climate change were simulated by following the guidelines provided by ARR 2016 (Ball, 2016). Future rainfall projections were obtained from the Representative Climate Futures Framework (CSIRO and Bureau of Meteorology, 2015). The changes in future rainfall intensity were derived by downscaling the results of a Global Circulation Model (GCM) for regional clusters of Australia. These projections were available for four Representative Concentration Pathways (RCPs) of future greenhouse gas and aerosol concentrations. Among the four RCPs, a low-emission scenario, RCP4.5 and a high-emission scenario RCP8.5 were used to test the impacts of future climate change on flooding in Marrickville.

Another factor that could affect patterns of flooding of MSR was the change in tailwater levels due to sea level rise. This is because the Cook River that flows through the Marrickville valley is connected to the Botany Bay coast (see Fig. 1e). A rise in sea level coupled with tidal influence can reduce the runoff from the upper catchment. To include this effect in our simulations, projections of sea level rise for Botany Bay were compiled (Jean Palutikofet al., 2017; New South Wales Government, 2005). Hence, four combinations of sea-level rise and rainfall increase were used in the simulations, as shown in Table 2, to estimate the 1% AEP design event.

3.6. Flood hazard index F_H

The Flood Hazard Index (F_H) was constructed for each SA1, for the base case and climate change scenarios, using four indicators generated from the TUFLOW flood simulations:

i. Extent of flooding as the ratio of flooded area to total area;
ii. Average maximum flood depth;
iii. Average maximum velocity;
iv. Average flood duration.

Any increase in any of the above-mentioned indicators increased the hazard index for the SA1. F_H was then used to classify each SA1 into one of five categories based on a subdivision of the index value into five equal intervals: a) lowest; b) lower; c) moderate; d) higher and e) highest. Any SA1 that is unflooded is allocated to the "lowest" category.

In addition to F_H, a flood categorisation adopted by the NSW government was generated from the results (New South Wales Government, 2005). It classifies each geographical unit of analysis as high hazard ("possible danger to personal safety; evacuation by truck difficult; able-bodied adults would have difficulty in wading to safety; potential for significant structural damage to buildings") or low hazard ("should it be necessary, truck could evacuate people and their possessions; able-bodied adults would have little difficulty in wading to safety"). Since the classification is based on flood depth and velocity only, its ability to predict impacts of flood is limited and is therefore referred to as "provisional hazard" by the New South Wales Floodplain Manual 2005 (New South Wales Government, 2005).

3.7. Exposure index F_E and social vulnerability index SoVI

Data about population density, overall building density and density of buildings constructed before 1980, was extracted for each SA1 from the National Exposure Information System (NEXIS), designed by Geoscience Australia (2019). The three indicators were used to build F_E.

The most comprehensive source of socioeconomic and demographic data in Australia is the Census data from the Australian Bureau of Statistics (ABS), collected and updated every five years. The Census data provides information on income, education, employment, occupation and housing, amongst others. The data was generated using information from persons, families or dwellings, at different spatial scales designed by the Australian Statistical Geography Standard (ASGS). The present study used data from the latest census (2011) available at the time of study.

The construction of SoVI involved a large number of socioeconomic

Table 2
Increase in Rainfall and Sea Level Rise Relative to 1985–2005 under Climate Change Scenarios.

Combination	RCPs and projected year	% of rainfall increase	Sea-level rise in Botany Bay (m)
1	RCP 4.5 (2060)	12	0.3
2	RCP 4.5 (2080)	12	0.42
3	RCP 8.5 (2060)	18	0.36
4	RCP 8.5 (2080)	18	0.56

and demographic variables. To reduce the number of variables to a manageable size, a multivariate statistical technique, the Principal Component Analysis (PCA) was applied. The reliability of the PCA decreases with decreasing sample size. Given the relatively small number of SA1s in MSR (84 SA1s), the PCA was conducted over a much larger study area (incorporating, but greater than, MSR), referred to here as the Broader Study Region (BSR). The BSR included the Inner West, Sydney City, Inner South and Sydney Inner South West and was made up of 2575 SA1s. Both MSR and BSR are shown in Fig. 1a.

Thirty-seven socioeconomic and demographic indicators (see Appendix A) were initially selected for the construction of SoVI based on a careful reading of existing literature, as discussed earlier in the section on social vulnerability. The indicators were compiled for the SA1s within BSR. Indicators that had high correlation (multicollinearity) or did not have any correlation with other indicators were then excluded from the analysis, with 16 indicators removed and 21 retained. Three tests were conducted on the retained indicators. First, the determinant of the correlation coefficient matrix was found to be 2.57×10^{-5}, greater than the minimum recommended value of 10^{-5}, confirming an acceptable level of multicollinearity (Field, 2009). Next, the Bartlett's test of sphericity was found to be highly significant ($p < 0.001$) implying that the correlation matrix of indicators was significantly different from the identity matrix and clusters could be identified. Finally, the Kaiser-Meyer-Olkin measure of sampling adequacy (KMO) was found to be 0.815, hence indicating that the PCA is likely to yield distinct and reliable components (Kaiser, 1970).

A cluster analysis was then conducted to identify major subgroups or components with eigenvalues greater than 1 using Kaiser's criteria (Kaiser, 1960). The scree plot was found to have a significant change of slope at component five. Hence, five components, which explained 66% of the variance, were selected. All 21 variables presented commonality extraction values greater than 0.5, which indicated that in all the variables, at least 50% of the variance was explained by the resulting principal component. The factor rotation technique (varimax orthogonal rotation) was applied to ensure that variables were loaded maximally to only one factor (Field, 2009). The index value of each social vulnerability component was determined by weighted summation of the standardised indicators values, with the weight taken as the absolute value of the rotated factor loading divided by the square root of the eigenvalue for a given indicator (Pink, 2013). Where indicators decreased with increasing vulnerability, the inverse of the indicator was used to ensure consistency in the direction of the relationship.

Two data analyses were then conducted. In data analysis 1, the indices of each component for each SA1 in MSR were converted to a 1 to 10 scale (from lowest to highest vulnerability), by normalising them relative to the minimum and maximum values of the index *within MSR*. In data analysis 2, the same procedure was followed but *normalising relative to the range of values within the bigger region BSR*. Hence, the first data analysis yielded an assessment of vulnerability of SA1s within MSR, relative to each other. The second data analysis provided an assessment of the vulnerability of MSR relative to the broader Inner-West and Inner-South region of Sydney. In both analyses, SoVI was calculated as the arithmetical sum of component scores, as described in Fig. 2b, and converted to a 1 to 10 scale, then five categories of vulnerability were extracted by subdividing SoVI into 5 equal intervals from "lowest vulnerability" to "highest vulnerability" (similar to the approach described for F_H earlier).

Finally, the sensitivity of the PCA to the choice of geographical region was assessed by generating a third region called MSR + . This was formed by expanding MSR to include a 2500 m buffer beyond all its boundaries. Hence, MSR + included 548 SA1s, compared to the 2575 SA1s in BSR. The PCA was then repeated, using MSR + instead of BSR, and the outcomes compared to the original analysis. Results were found to have relatively low sensitivity to this change in the size of the geographical area. In both analyses (BSR and MSR +), 21 indicators were retained, 19 of which were the same and had comparable explanatory power.

The "Statistical Package for the Social Sciences" (SPSS) was used to analyse demographic and socioeconomic data, perform the PCA and construct the social vulnerability index (Field, 2009). The GIS tools ArcGIS and QGIS were used for processing, analysing and mapping model data.

4. Results

4.1. Flood simulation under base case

The DRAINS model was used to simulate ensemble storms (storm pattern 1 to 10, discussed earlier under flood modelling) with different storm durations, from 1 to 24 h for the 1% AEP. The aim was to identify the critical duration producing the highest flow. The maximum median peak flow (44.8 m^3/s) occurred for a 1-hour storm duration and a storm scenario with equal peak flow was taken as the design storm for 1% AEP, for the base case. Flood simulation results for the base case are shown in Fig. 3.

According to simulations, a total of 17.6% of the MSR surface area is flooded under a 1% AEP design storm event. Approximately 10% of the surface area of the MSR is under 0.1 to 1 m of flood depth, with low water velocity (<= 0.4 m/s). A small surface area (0.6%), made mostly of the Marrickville Oval Stadium, is highly flooded (depth greater than 1 m). On the other hand, areas falling under high velocity (>= 2 m/s) are mostly roads. The maximum flood duration due to 1% AEP for this region is 3 h. Unsurprisingly, the areas that are more deeply flooded (see Fig. 3a) are also found to be flooded for longer (see Fig. 3c).

The provisional hazard map (Fig. 3d) for the MSR represents the combined effects of flood depth and velocity. Most of the MSR (82.4%) is safe from flooding. Most flooded areas fall in a low-hazard category (15.8% of MSR or 90% of flooded area). The remaining part (1.8% of MSR or 10% of flooded area) is a high-hazard zone and includes, as expected, the Marrickville Oval Stadium and several roads towards the south of MSR.

Table 3a summarises the flood characteristics under the base case and Fig. 4a shows the distribution of F_H. Among the 84 SA1s experiencing flooding, thirty-four fall into categories of higher to highest vulnerability. The outcome is consistent with the findings, discussed above, about the four individual variables of depth, velocity, duration and extent. For example, SA1 identified as number 1 in Fig. 4, includes the Marrickville Oval and experiences flood depths higher than 1 m, and flood durations between 2.5 and 3 h. These values are close to the maximum values for the base condition. Though the average flood velocity in this SA1 seems low (0 and 0.4 m/s), 49% of the surface area of this SA1 is flooded, a proportion close to the maximum of 56%. Hence, the comparatively large values of at least three of the four indicators point to high levels of hazard for this SA1 as reflected by F_H. A similar reasoning can be applied to SA1s marked as 2 and 3 in Fig. 4a.

4.2. Flood simulations under climate change

Flood simulations under climate change were conducted as variations on the base case, as shown by the combinations of rainfall and tailwater rise in Table 2. Contours of peak flood depth, peak velocity and flood duration under the more severe climate change scenario (RCP8.5–2080) are shown in Fig. 5, both in absolute value and relative to the base case scenario. Results for the other climate scenarios were found to differ from RCP 8.5, 2080, in values but not in overall patterns. Consequently, they are not shown here but can be found in (Ahmed, 2018). Fig. 6 shows the provisional hazard categories under climate change scenario RCP8.5, as well as the change in these categories relative to the base case. A comparison of the percentages of area flooded under different flood indicators due to the base case and the more severe CC scenario (RCP 8.5–2080) is shown in Table 3a. Statistics of flood hazard zone classification for base case and CC scenario are compared in

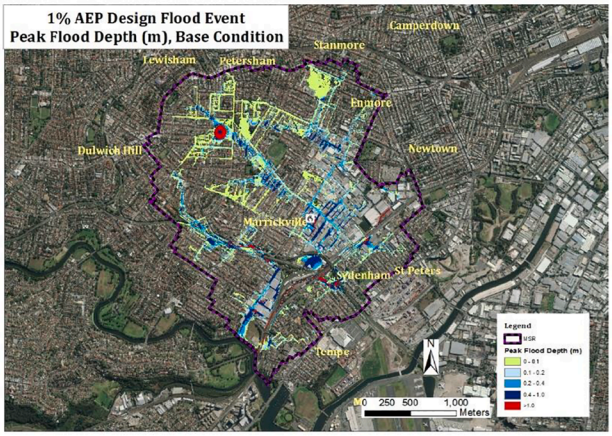

a. Peak flood depth

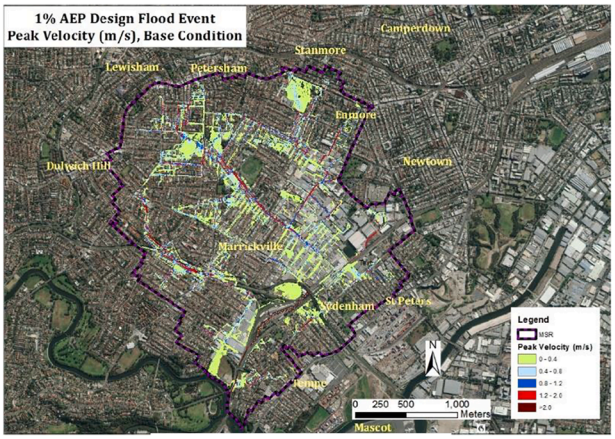

b. Peak velocity

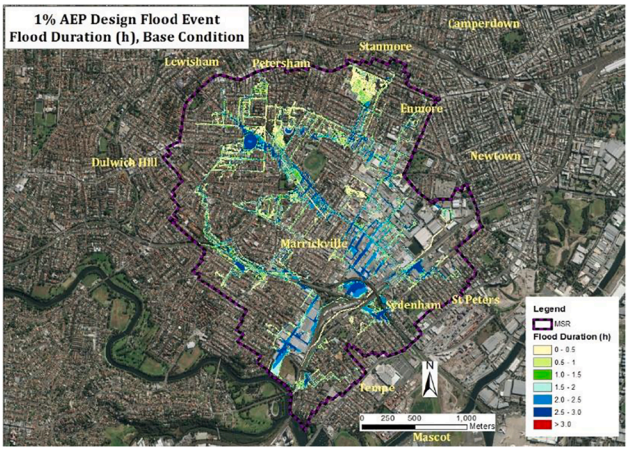

c. Flood duration

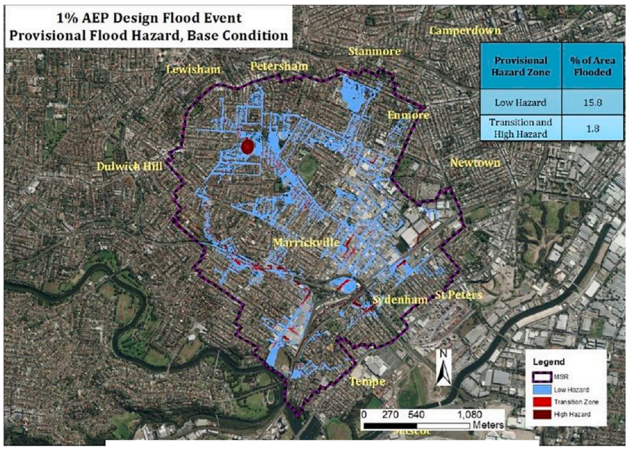

d. Provisional flood hazard

Fig. 3. Flooding patterns for base case (1% AEP design storm event for 1-hour duration).

Table 3
Percentage of area flooded under different flood depths, velocities and durations for base case and climate change (CC) scenario RCP8.5–2080.

a. Flood depth, velocity and duration

Area Flooded Under Different Flood Depth Zones			Area Flooded Under Different Velocity Zones			Area Flooded Under Different Flood Durations		
Flood Depth (m)	Area Flooded as % of MSR		Flood Velocity (m/s)	Area Flooded as % of MSR		Flood Duration (h)	Area Flooded as % of MSR	
	Base	CC		Base	CC		Base	CC
0–0.1	7.3	7.4	0–0.4	9.8	10.4	0–0.5	3.9	3.9
0.1–0.2	3.2	3.2	0.4–0.8	4.0	4.5	0.5–1	2.5	2.2
0.2–0.4	3.6	3.9	0.8–1.2	2.0	2.3	1–1.5	2.3	1.2
0.4–1	2.8	4.0	1.2–2.0	1.4	1.8	1.5–2	2.2	0.7
greater than1	0.6	0.9	greater than2	0.3	0.5	2–2.5	2.8	0.5
–	–	–	–	–	–	2.5–3	3.8	1.2
–	–	–	–	–	–	greater than 3	0	9.6

b. Provisional flood hazard categorisation

Scenario	Area flooded as % of total MSR area	Low-hazard zone as % of total MSR area (as % of flooded part of MSR)	Transition- and high-hazard zone as % of total MSR area (as % of flooded part of MSR)
Base	17.6%	15.8% (90%)	1.8% (10%)
RCP 4.5 (2060)	19.3%	16.4% (85%)	2.9% (15%)
RCP 4.5 (2080)	19.3%	16.4% (85%)	2.9% (15%)
RCP 8.5 (2060)	19.3%	16.4% (85%)	2.9% (15%)
RCP 8.5 (2080)	19.4%	16.4% (85%)	2.9% (15%)

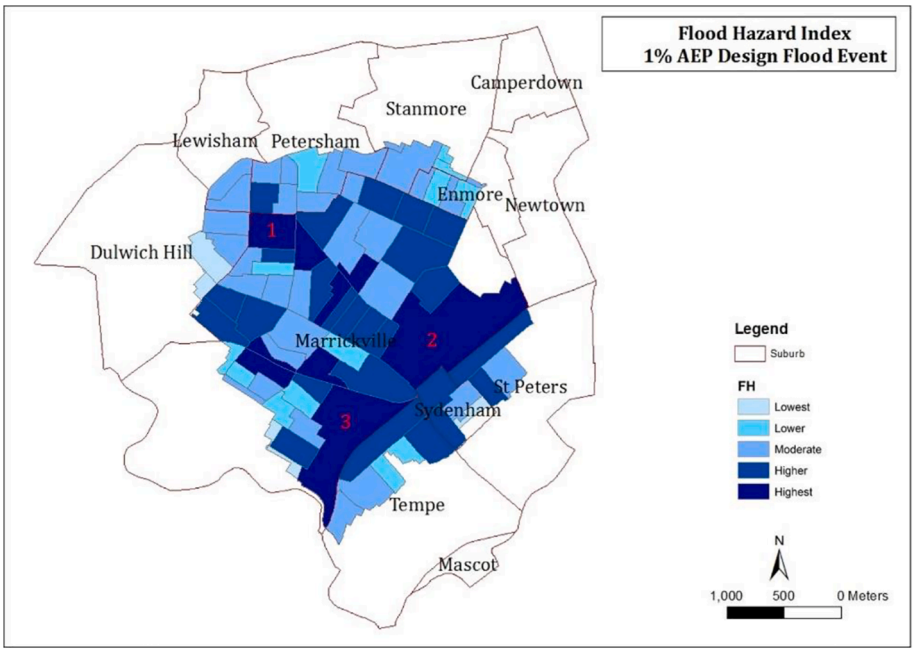

a) Under Base Case

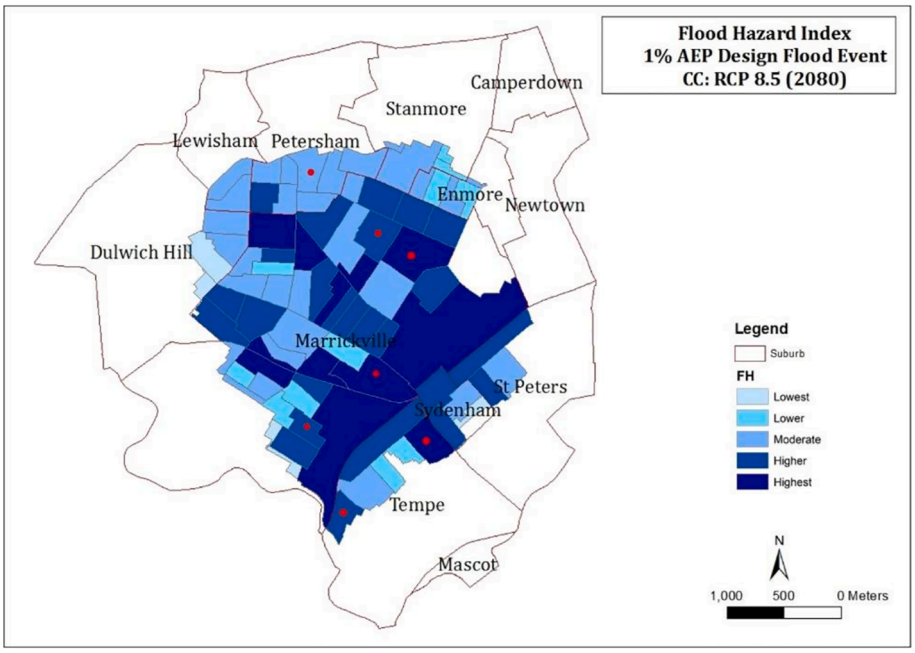

b) Under RCP 8.5 (2080)

Fig. 4. Flood Hazard Index under Base Case and Climate Change Scenario RCP 8.5 (2080).

Table 3b.

Under RCP 8.5, 2080, extent of flooding increases from 17.6% (base condition) to 19.4%. No significant differences are observed between the various RCP's for years 2060 and 2080, i.e. the percentages of flooding area are stable at around 19.4% (Table 3b). Fig. 5a and 6b reveal that an additional area of around 2% of MSR is flooded as a result of climate change, mostly in the vicinity of Cooks River due to the tailwater effect. In comparison to the base condition, flooding depth increases by up to 0.2 m and mostly within the area where flooding extent has increased (Fig. 5a and 5b). In addition, an increase in velocity by 0.2 m/s is seen in some areas (Fig. 5c and 5d). Nowhere in MSR is flood depth reduced, but velocity is projected to decline in around 2% of the MSR, under RCP 8.5, 2080. The change in water velocity under climate change scenarios is the net outcome of two counteracting effects: a) the increase in rainfall which increases water pressures, hydraulic gradients and hence water velocities and b) the rise in sea levels which reduces hydraulic gradients and hence water velocities.

The maximum flood duration is projected to increase to up to 7 h, compared to 3 h under the base case (Fig. 5e). Even more significantly, the percentage of land in MSR experiencing flooding for more than 3 h rises from nil under base case to close to 10% under climate change RCP 8.5, 2080 (Fig. 5e and Table 3a). This is mainly due to sea level rise in

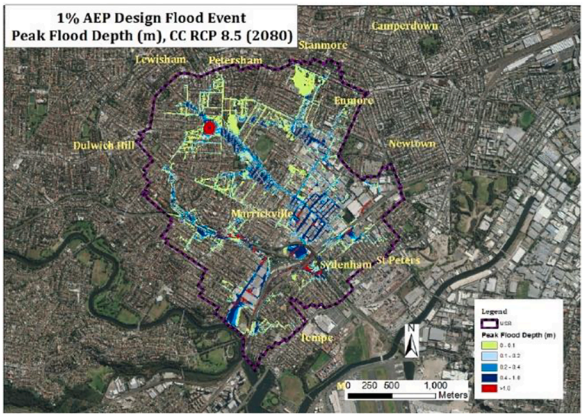

a. Peak depth

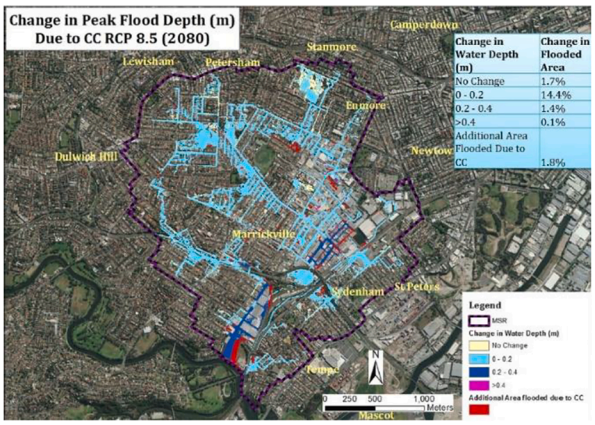

b. Change in peak depth relative to base case

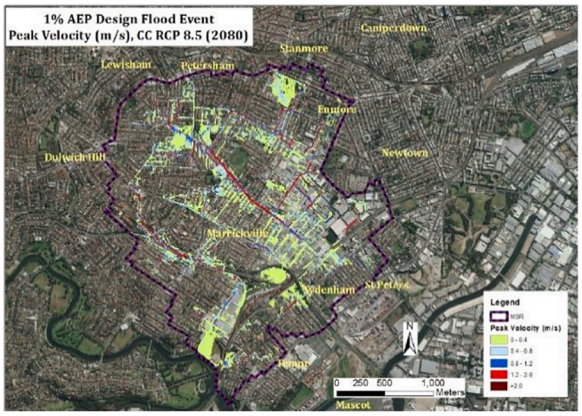

c. Peak velocity

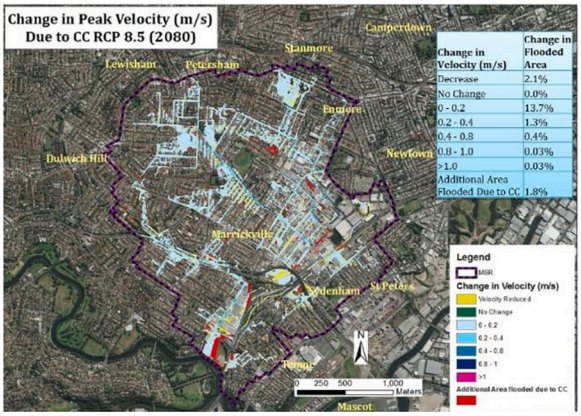

d. Change in peak velocity relative to base case

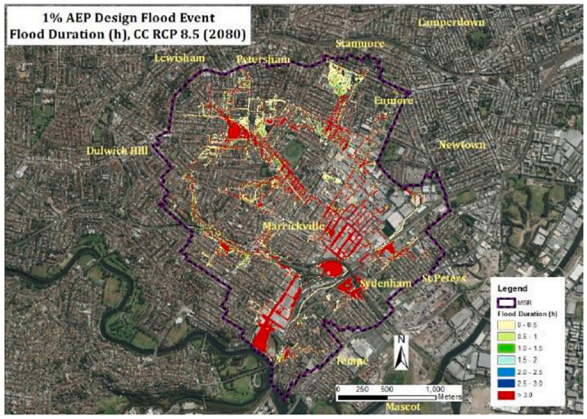

e. Duration

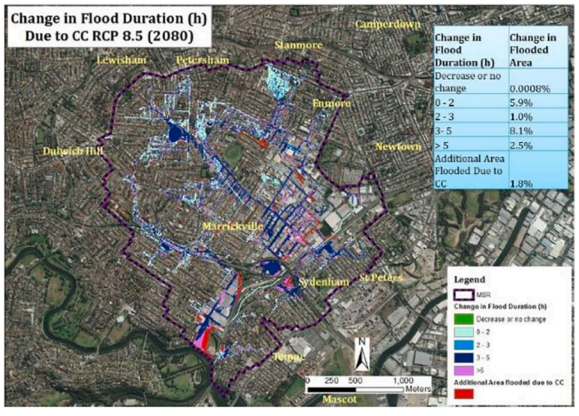

f. Change in duration relative to base case

Fig. 5. Flooding patterns for climate change scenario, RCP 8.5, 2080 (1% AEP design storm for 1-hour duration).

the Cook River which slows down drainage of runoff water.

For most of the MSR, there is no change in provisional hazard categories due to CC (Fig. 6a and 6b). The additional 2% of flooded areas under climate change falls in the low-hazard category. However, as shown in table 3, the percentage of total MSR area falling in the transitional and high-hazard categories has increased to 15%, from 10% under base-case scenario. Fig. 4b shows the new spatial distribution of F_H under RCP 8.5, 2080. The hazard in only 7 SA1s (marked with a red dot in Fig. 4b) increases to the next higher level, under RCP8.5 compared to the base case. This does not necessarily mean that vulnerability of other SA1s hasn't increased, just not severely enough to move to the next hazard category.

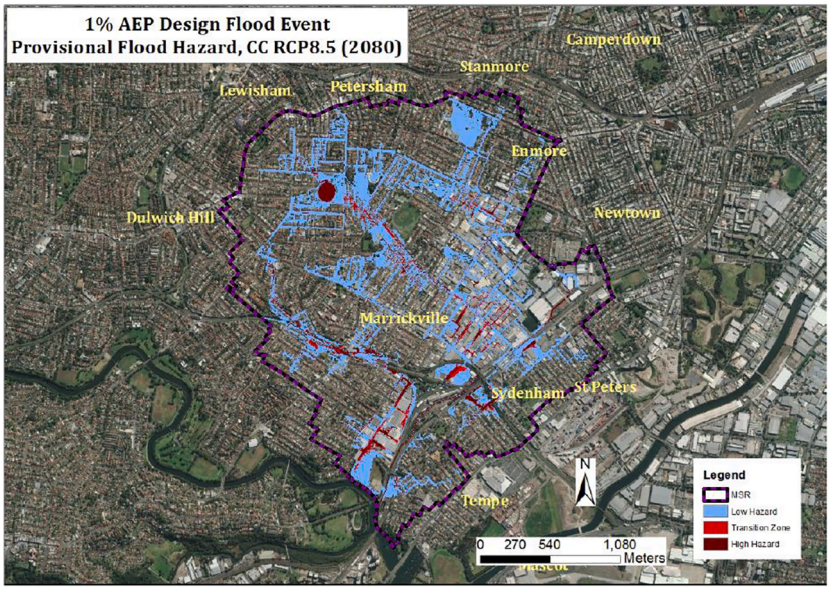

a. contours of provisional hazard categories

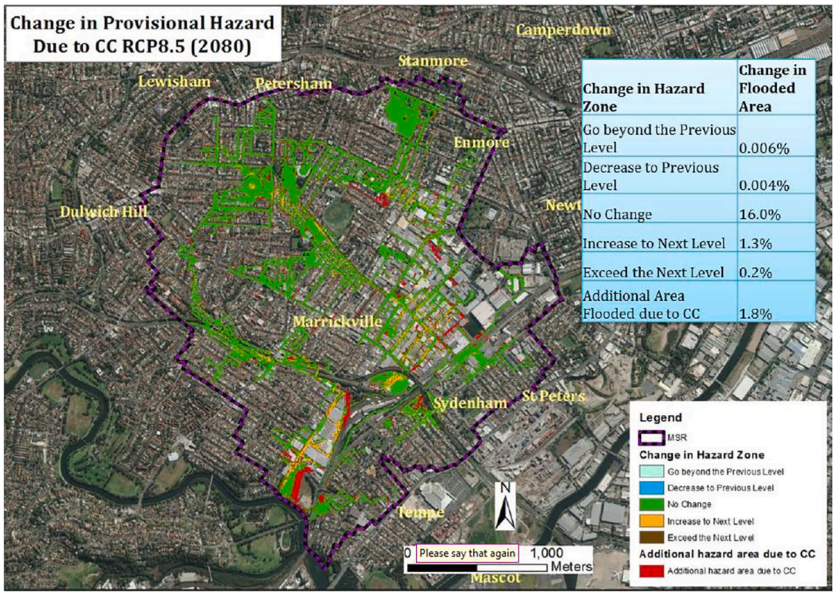

b. contours of change in provisional hazard categories relative to base case

Fig. 6. Provisional hazard categories under climate change RCP 8.5–2080.

4.3. Population and building densities

Fig. 7 shows the variation of F_E, discretised into five categories of exposure, from "lowest" to "highest". The region of reference is the MSR itself in Fig. 7a, and BSR in Fig. 7b. In Fig. 7a, several SA1s in and around Enmore, Lewisham, Dulwich Hill and Marrickville have high exposure, on account of high residential density. SA1s between Marrickville and Sydenham have very low exposure because of the predominantly industrial nature of the area. When the larger BSR is taken as a reference, Fig. 7b reveals high or very high exposure in around twenty SA1s, none of which is in MSR.

4.4. Social vulnerability

The five extracted principal components for MSR from SoVI analysis 1 are detailed in Table 4. Fig. 8 shows the spatial distribution of SoVI, as well as individual components. It indicates that higher social vulnerability occurs mostly within the western part of the MSR, due to several factors. For example, the SA1s marked as 1 and 2 in Fig. 8 are classified as socially vulnerable as a result of scores for component 1 (household structure, English proficiency and schooling) and 4 (age structure) but NOT components 2 (immigration status and income), 3 (property rental/ownership and unemployment) and 5 (education). Specifically, in these two SA1s, there is a relatively large proportion of dwellings occupied by more than 5 individuals or more than 1 family, single and/or aged individuals and/or individuals with low English proficiency. On the other hand, the social vulnerability of SA1 marked as 3 in Fig. 8 is due to high proportions of migrants, low-income households and individuals with lower educational levels. Conversely, the SA1s in the eastern part of the MSR, marked as 4 and 5, rank low on social vulnerability mainly because of the predominantly industrial land use and the low number of residential dwellings in those parts of MSR.

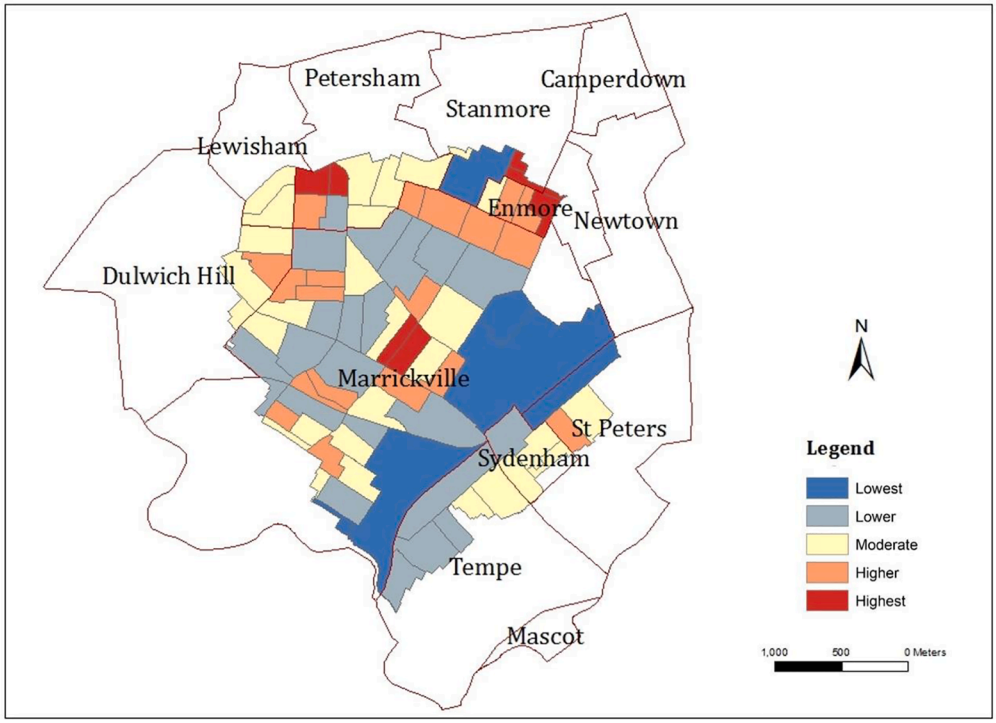

a) with Marrickville valley as the region of reference

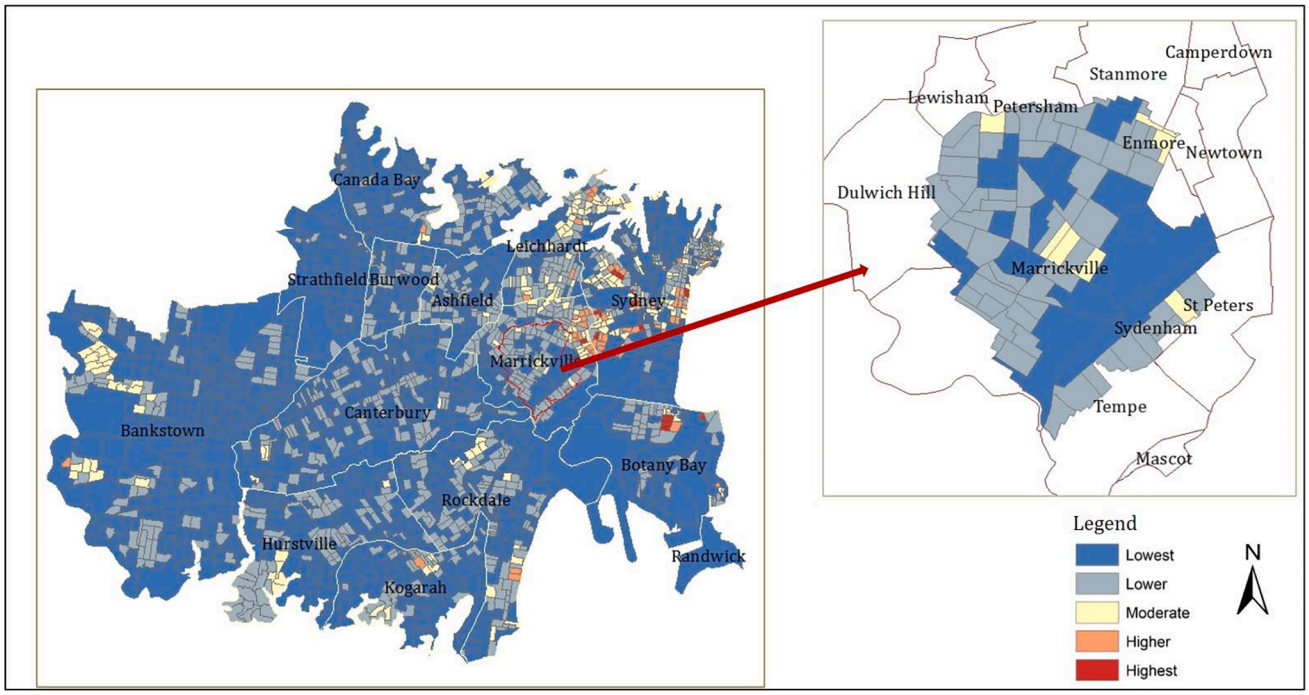

b) with the Inner West at the region of reference

Fig. 7. Exposure index within Marrickville valley.

Fig. 9 shows social vulnerability of MSR (84 SA1s) as it emerges from data analysis 2 with the larger BSR taken as a reference, i.e., relative to MSR's larger Inner-City context. The figure indicates that although some SA1s in the western part of Marrickville have relatively high social vulnerability, the most socially disadvantaged SA1s fall in the Inner-West around Bankstown and Canterbury, rather than Marrickville.

Table 4
Extracted Principal Components of Social Vulnerability Indicators from SoVI Analysis 1 for MSR (66% of variance explained; determinant of correlation matrix = 2.57×10^{-5}; Bartlett's test of sphericity: $p < 0.001$; KMO = 0.815).

Principal Component	Eigen Values	Indicators	Factor Loading after rotation
1 Household structure, English proficiency and schooling	5.157	Number of dwellings occupied by 5 individuals or more	0.773
		Number of household with 2 or more families	0.726
		Number of dwellings occupied by single individuals	-0.655
		Number of people with low speaking proficiency in English	0.630
		Number of couple families with more than 2 dependent children	0.623
		Number of people who never went to school	0.605
2 Immigration status and income	3.536	Number of non-citizens	0.843
		Number of households with negative or nil income	0.747
		Number of recent migrants (previous 8 months)	0.743
		Number of people with weekly negative or nil income	0.706
		Number of houses with weekly rent over the median household rent	0.542
3 Property rental/ ownership and unemployment	2.425	Number of houses with weekly rent below $150	0.812
		Number of single-parent families with children under 15	0.633
		Number of unemployed families	0.575
		Number of dwellings owned with mortgage	-0.562
		Number of dwelling owned outright or being purchased	-0.500
4 Age Structure	1.724	Number of people over 65 years of age	-0.741
		Number of people between 35 and 39 years	0.685
		Number of children below 5 years of age	0.531
5 Education	1.013	Number of people whose highest level of education is year 11	0.814
		Number of people whose highest level of education is Certificate Level (Certificate 1, 2, 3 or 4)	0.508

4.5. FSVI mapping

The three indices F_H, F_E and SoVI were combined additively and multiplicatively to construct FSVI as described earlier. No correlation was found to exist between the three indices hence confirming that useful information on hotspots can be elicited by overlaying them through aggregation. As expected, Fig. 10 shows that, under multiplicative aggregation, only SA1s with high values on all 3 indices are given high FSVI values.

To examine how different indices contribute to the FSVI, four SA1s (A_1, A_2, A_3 and A_4 shown Fig. 10) with different FSVI categories (low, medium, high and very high, respectively) are selected from the results generated with additive aggregation. The individual indicator/component score producing of F_H, F_E and SoVI are shown in Table 5. All selected SA1s have High or Very High F_H, indicating geophysical susceptibility to flooding. A1 has high population density, and high buildings density, a relatively large proportion of which is old building stock. This leads to a high value of F_E. In addition, A1 has relatively high scores for principal components of social vulnerability. In A2, densities of population, buildings and old buildings are comparatively low and SoVI is one level lower, leading to an FSVI that is one level lower than A1. Area A3 is located in a largely industrial zone with no old buildings, and only a small proportion of residential properties. This leads to low F_E and SoVI and, therefore, despite the high F_H, low overall vulnerability reflected by a low FSVI. Finally, the vulnerability level of A4 is moderate, with high social vulnerability but low exposure index.

4.6. Focus group with municipal council stakeholders

The research project was conducted in collaboration with the Inner-West Council, which is the municipal authority responsible for the MSR, including land use and flood management. At the beginning of the project, a meeting was conducted at the Council's Office to discuss the project brief (27th July 2016). The Council provided part of the data required for flood simulations. A 90-minute meeting was then organised (24th August 2017) at the Council's Office attended by, in addition to the first and second authors, three Council staff, namely the Coordinator of Asset Planning, a Development and Planning Engineer and a Design and Planning Engineer. The researchers presented the project's objectives, methodology and outcomes followed by extensive discussions and responses by Council staff.

The meeting yielded two important insights by Council staff about the usefulness of the study. First, Council staff saw a good potential for the findings of the research project to inform existing Council's flood management process. The study findings were considered especially useful for the flood emergency response services. Combining geophysical, built environment and social vulnerability data was deemed to provide information not usually available to emergency services, and to help in developing better contingency plans. This is particularly pertinent in light of the marked increase in flood duration under RCP 8.5 – 2080. Second, one of the limitations of the social vulnerability index, noted by Council staff, is that it is based on household survey data by the Australian Bureau of Statistics, which does not capture the vulnerability of employees of workplaces located in Marrickville. Different kind of data would be required to develop a map of workplace vulnerability, including, amongst others, number of employees, firm assets and resources, and the adequacy of emergency procedures in place at the firms. This was beyond the scope of this project.

5. Discussion

5.1. Vulnerability to flooding

Analysis of vulnerability to climate stressors combines two approaches to environmental risk, one of which is much more recent than the other. Space-time heterogeneities have long been recognized as fundamental for understanding ecological dynamics and the resilience of socio-ecological systems to environmental stressors (Levin and Levin, 1989; Convertino and Valverde, 2019). From this perspective, computational modelling can unveil key dynamics underlying hazards and exposure to them. In particular, the spatial downscaling of predictions of global circulation models of climate change, when combined with hydrological accounts of flood patterns at neighbourhood scale, can produce a more refined, place-specific understanding of floods and their variabilities in space and time (Willems et al., 2012; Loaiciga et al., 1996). On the other hand, socio-economic disadvantage underlying differential exposure to risk is increasingly recognised as a key driver of vulnerability to ecological stress (Adger, 2000; Berkes et al., 1998; Satterthwaite, 2003). The spatial mapping of social inequalities has hence become a key element in understanding environmental risks,

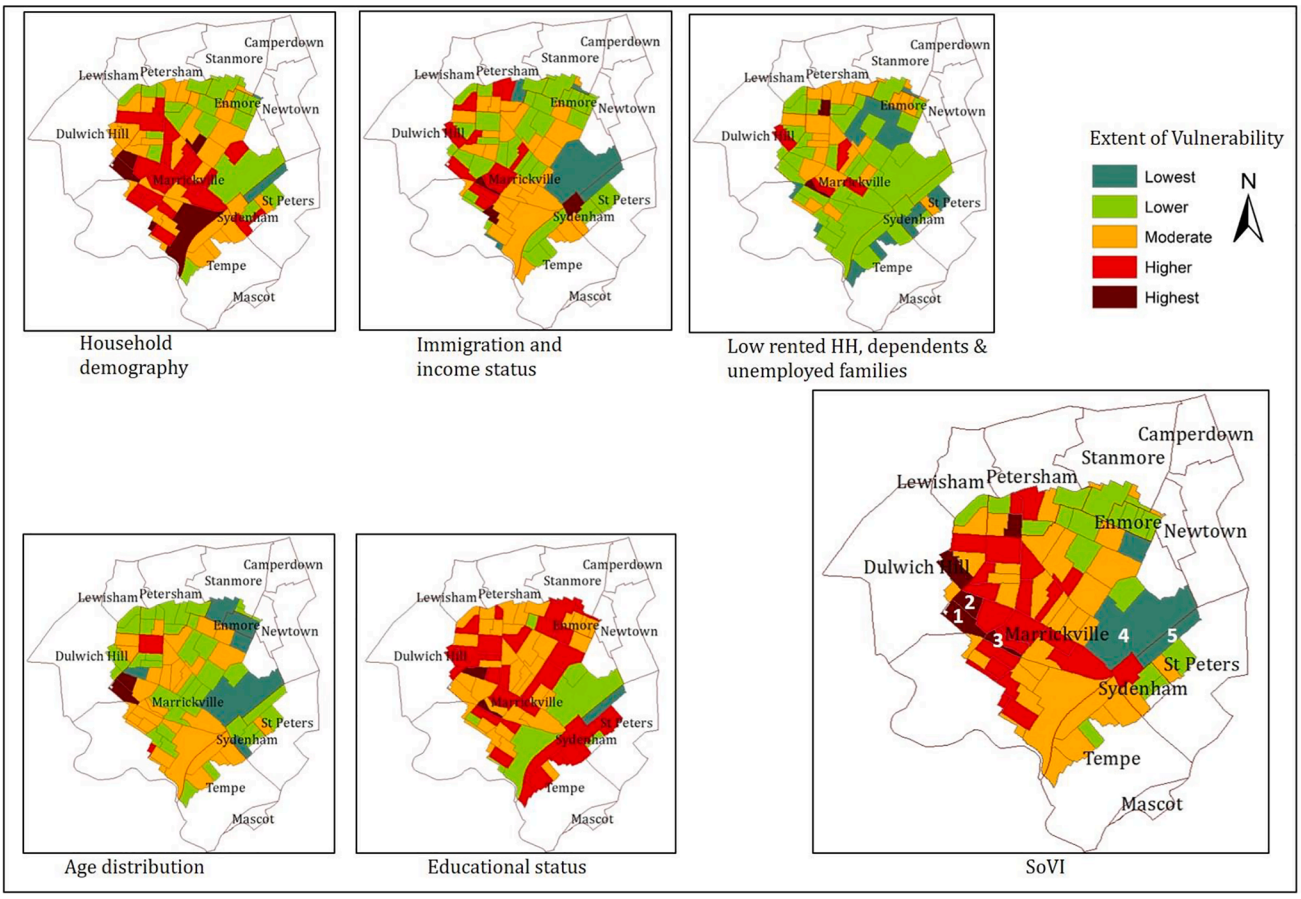

Fig. 8. Spatial distribution of SoVI in MSR, including distribution of individual components.

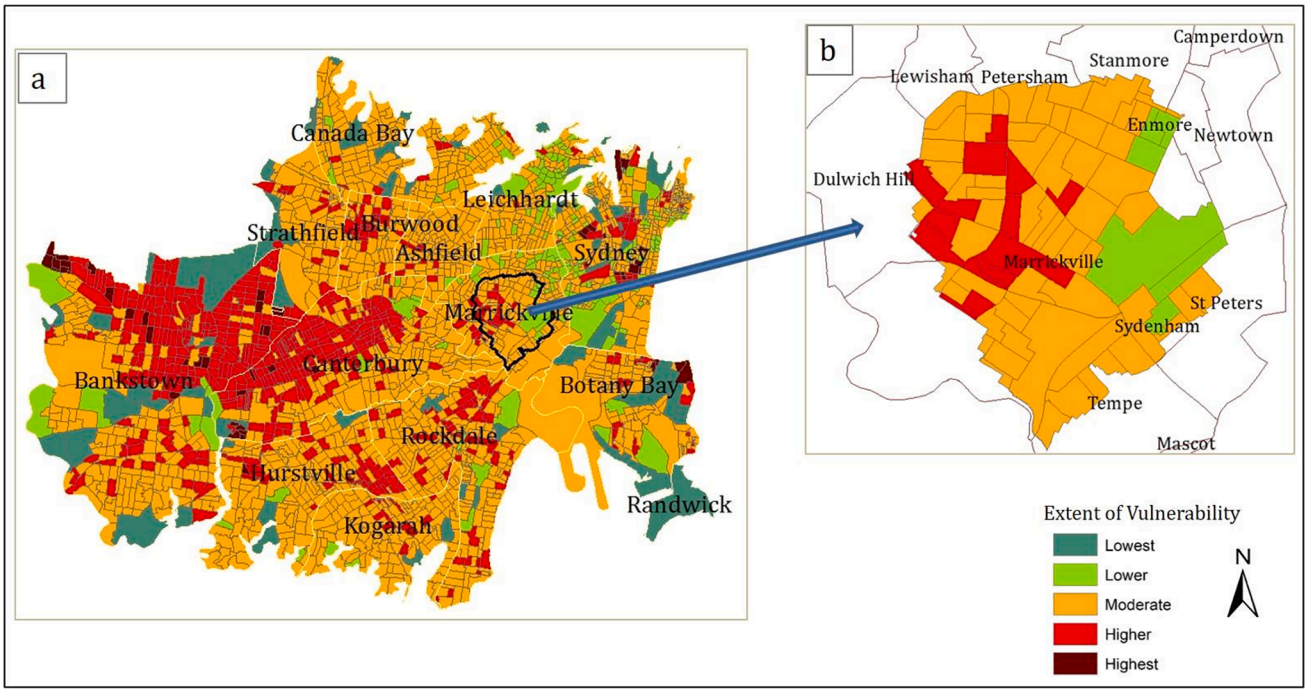

Fig. 9. SoVI for Larger Geographical Area of BSR (data analysis 2).

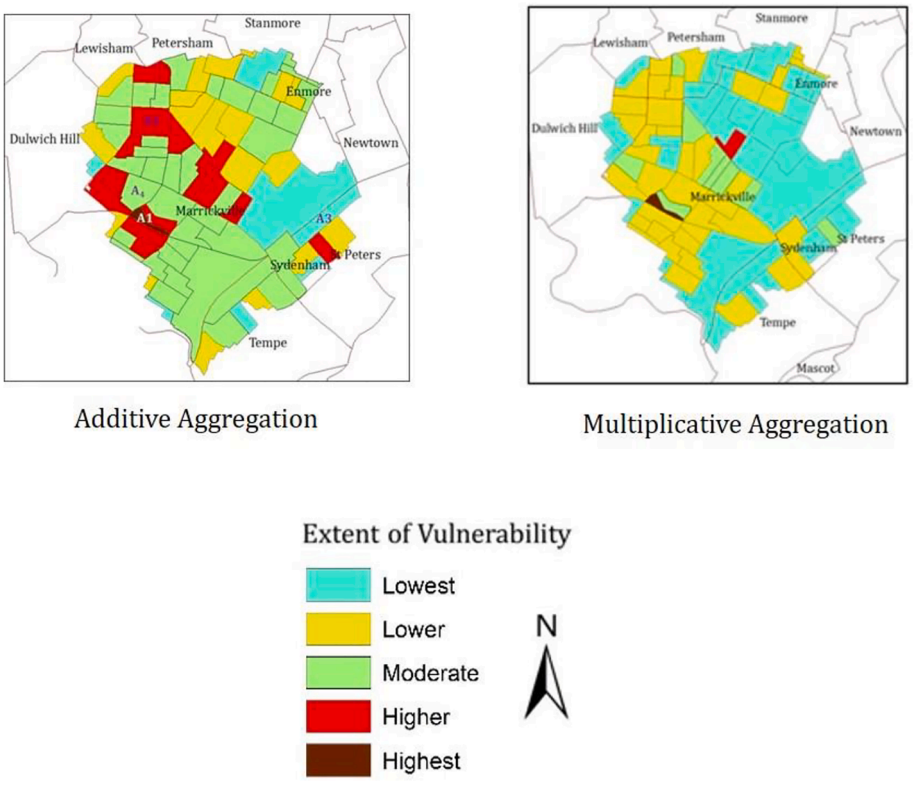

Fig. 10. Distribution of FSVI by Additive and Multiplicative Aggregations.

Table 5
Comparison of Indicators for Four Selected SA1s (the location of the four SA1s, A1, A2, A3 and A4, are shown in Fig. 10).

Indices	FSVI category Indicators	A_1 (Residential) Highest		A_2 (Residential & parkland) Higher		A_3 (Industrial) Lower		A_4 (Residential) Moderate	
Flood Hazard Index	Mean Flood Depth (m)	0.31	Highest	0.37	Highest	0.35	Highest	0.12	Highest
	% of Flooded Area	0.56		0.49		0.16		0.04	
	Flood Duration (h)	1.53		1.62		1.99		1.51	
	Flood Velocity (m/s)	0.78		0.45		0.38		1.10	
Flood Exposure Index	Population density (/km^2)	7954	Highest	3395	Lower	57	Lowest	5149	Lower
	Building density (/km^2)	1525		1039		97		1418	
	Old building density/sq km	449		64		0		73	
Social Vulnerability Index	Component 1	5.8	Highest	6.9	Higher	1.0	Lowest	7.6	Higher
	Component 2	9.0		4.1		1.5		4.0	
	Component 3	8.9		6.2		4.6		5.4	
	Component 4	5.0		6.8		3.4		4.7	
	Component 5	8.9		8.2		1.0		5.6	

including those generated by floods (Fielding and Burningham, 2005). Vulnerability assessments is a semi-quantitative means of combining the above two approaches to generate refined knowledge-based data that can assist in policy making on reduction of vulnerability to floods.

5.2. *Change in flood patterns under climate change*

Two different greenhouse gas emission scenarios (low and high emission scenario RCP4.5 & RCP8.5) were used to predict future physical characteristics of floods in MSR for the years 2060 and 2080. The aim of the study was to predict the effects of climate change on vulnerability to flooding in MSR, under current socio-economic, demographic and built-environment conditions. While this approach has been followed in several other studies (Ahmed, 2018; Schreider et al., 2000; Ashley et al., 2005; Zhou et al., 2016), its main drawback is that urban expansion, which has been identified as an important driver of future flood risk in a number of climate change studies, was not taken into account here (Berggren et al., 2011; Muis et al., 2015).

Our modelling showed worsening of flooding in the study area, which is broadly consistent with findings in the literature (Ahmed, 2018; Zhu et al., 2007; Zhou et al., 2016; Chang et al., 2009; Ahmed et al., 2018). Specifically, a significant increase in the duration of floods under climate change was predicted, but only limited change in other flood hazard indicators such as flood depth and velocity. The increase in flood duration is due to sea level rise which slows down discharges by the urban drainage system of MSR into the Cooks River. More protracted floods have been found to cause more damage (Kelman and Spence, 2004; Soetanto and Proverbs, 2004). During the last few decades, the average annual flood duration along the U.S. East Coast has been increasing due to sea level rise (Ezer and Atkinson, 2014). Longer flood durations can lead to higher dependency on emergency services, higher costs of emergency and longer recovery times for the community. Another implication of this finding is that, if the bottleneck to drainage occurs downstream, increasing the drainage capacity through infrastructural change may not address the problem and resources may be better directed at improvement of flood warning and better access to

flood-affected communities. This is clearly an open question which deserves more research.

Significantly, the NSW Flood Plain Manual (FPM) categorises flood hazards based on flood depth and velocity, but *not* flood duration. This was reflected in our analyses when, 85% of flooded areas of MSR under CC was categorised as low hazard, compared to 90% under the base case, despite the increase in flood duration under CC. This is due to lower velocities under CC. Although flood duration is likely correlated to flood depth, the latter is unlikely to capture the full effects of the former. Hence, our findings suggests that there may be a case for revising this categorisation in order to include flood duration, as well as place-specific vulnerability assessments.

5.3. Flood indices

Planning for urban flooding has been traditionally based on geophysical assessment of flooding patterns at city scale (Muis et al., 2015; Jongman, 2015). The literature on vulnerability and environmental risk emphasises that impacts of extreme weather events are experienced differently by different segments of the population, depending on socio-economic, demographic, institutional and built–environment factors (Zahran et al., 2008; Cutter et al., 2013; Jongman, 2015). Several attempts at combining socio-economic and geophysical elements of flooding have been attempted in the literature (Tavares et al., 2015; Garbutt et al., 2015; Koks et al., 2015) including construction of composite indices (Connor and Hiroki, 2005; Balica and Wright, 2012; Zachos et al., 2016). However, very few attempts have been made at building such indices using fine-scaled hydrological-hydraulic modelling and municipal data and aiming to compare units within one municipality rather than between different municipalities. Hence, the modalities and usefulness of such an exercise remain an open question.

The three components of FSVI developed here were found to be poorly correlated when applied to the Marrickville Study Region (MSR), hence lending support to the hypothesis that such an index may yield additional information, not provided by its individual components. The possibility of a strong correlation between the three components arises from the fact that the economically and/or politically disenfranchised often occupy environmentally marginal land and are hence more exposed to the impacts of pollution and extreme weather events (Pulido, 2000; Satterthwaite, 2003; Adger, Aug., 2006). However, this is not always the case, as Cutter et al. (Cutter et al., 2000) have argued, and the most vulnerable places from the biophysical viewpoint do not always overlap with the most vulnerable populations. In the case of MSR studied here, no consistent pattern relating the three components of risk has been found, with some areas of MSR identified as susceptible to flooding, scoring low on social vulnerability, while other socially vulnerable areas are found to be at low risk of flooding. Indeed, the study has found that the FSVI exhibits significant spatial variations within MSR especially in relation to its hazard and social vulnerability components. This is aligned with previous research on social vulnerability (Cutter et al., 2003; Holand et al., 2011; Tavares et al., 2015; Garbutt et al., 2015; Koks et al., 2015).

5.4. Role of vulnerability studies in flood policy making

Our findings suggest that combining information about the physical characteristics of flood with local-scale data on social vulnerability and built environment allows flood mitigation efforts to be targeted at the most vulnerable segments of the population. It can bring to the portfolio of flood adaptation actions a set of targeted, non-infrastructural measures that are often low-cost. Examples include increasing flood awareness amongst migrants, new residents and/or those with low levels of education and minor retrofitting to waterproof old buildings (Cutter et al., 2003; Koks et al., 2015). The data can further be used by emergency services to predict the recovery capacity of various localities and flood evacuation plans can hence be tailored and prioritised, targeting those with low mobility and low access to resources. Cutter et al. (Cutter et al., 2003) pointed out that resource prioritisation for flood mitigation may be vulnerable to politics of vested interests. Data, such as those developed in this study, can help in providing an objective basis for discussions between stakeholders attempting to develop collective action on flooding.

A question remains, nevertheless, as to whether vulnerability studies actually feed into policy processes for flood mitigation. Critiques from political science literature have argued that vulnerability studies do not consider policy context and are not action-oriented, which limits their usefulness (Wellstead et al., 2013; Wise, 2014). Examining studies of vulnerability to heat waves, Wolf et al. (Wolf et al., 2015) concluded that they have not had “a substantive influence on policy-making or preventive action”. In a review of the literature on vulnerability, Ford et al. (Ford et al., 2018) found that, although 44 studies raised this question, there was a dearth of papers providing empirical evidence in addressing it.

The policy context of our own study is partly determined by the state government of New South Wales which requires local councils to develop their own sea level rise planning and to adopt their own, place-specific sea level rise projections. The NSW Flood Pain Manual (FPM) recommends that any flood mitigation measure consider, in addition to cost-benefit aspects, criteria of social feasibility and impacts. However, no mention is made of socio-economically differentiated impacts and vulnerabilities. This manual is prepared to assist the local government in formulating flood management plans through the flood risk management process. The first step of this process is to set up a Floodplain Risk Management Committee whose objective is to assist the local authority in the development and implementation of a flood plain risk management plan. A Flood Management Advisory Committee (FMAC) advises the Inner West Council (which oversees flood management in MSR). This is a discussion forum which includes technical, social, economic and environmental matters and whose recommendations are usually adopted by the Council. Hence, discussion, adoption and/or dissemination of (parts of) the study’s findings by the FMAC would be the most effective route by which the vulnerability assessment reported here may have an impact in actual flood policy. Preliminary feedback by Council stakeholders, as mentioned earlier, is encouraging and appears to suggest that data generated by the locally specific assessments may feed into adaptation measures and policies. However, whether such an adoption will take place in the future remains to be seen.

6. Conclusions

The paper has proposed and implemented a methodology for combining hydrological-hydraulic modelling and social vulnerability assessment at local municipal scale in order to evaluate vulnerability to flooding under climate change. The exercise has yielded a richer set of data that appears to be useful for planning purposes of municipal government.

Several lines of investigation can be pursued as extension of this research. First, the hydraulic/hydrological analyses can be incorporated within a more complete probabilistic framework in order to generate probability distribution functions of flood indicators. The shape of these functions can help in understanding the modalities and persistence of flood risk and, through global uncertainty and sensitivity analyses (GSUA), in better characterising global sensitivities of vulnerability to floods (Saltelli et al., 2004; Convertino et al., 2018).

Second, refining future projections of vulnerability so as to incorporate the effects of urban change, including economic growth and population dynamics, and not just climate change, is vital for a better understanding of future floods.

Third, observing how this vulnerability assessment, and others, are received by policy-making agencies and how this reception evolves over time would yield valuable information about critical research-policy

interfaces in adaptation to climate change.

CRediT authorship contribution statement

Abbas El-Zein: Conceptualization, Funding acquisition, Investigation, Methodology, Project administration, Resources, Supervision, Writing - original draft, Writing - review & editing. **Tanvir Ahmed:** Conceptualization, Data curation, Investigation, Formal analysis, Methodology, Resources, Software, Validation, Visualization, Writing - review & editing. **Fahim Tonmoy:** Methodology, Supervision, Visualization, Writing - review & editing.

Declaration of Competing Interest

The authors declare that they have no known competing financial interests or personal relationships that could have appeared to influence the work reported in this paper.

Acknowledgements

We thank the Inner West Council for collaborating on this research, providing data and feedback. We are grateful for feedback on the early parts of this study by Dr Federico Maggi and Dr Ken Chung. The project has been partly funded by a research grant from the School of Civil Engineering of the University of Sydney.

Appendix A. Supplementary data

Supplementary data to this article can be found online at https://doi.org/10.1016/j.ecolind.2020.106988.

References

Jongman, B., et al., 2015. Declining vulnerability to river floods and the global benefits of adaptation. Proc. Natl. Acad. Sci. 112 (18), E2271–E2280.
Hallegatte, S., Green, C., Nicholls, R.J., Corfee-Morlot, J., 2013. Future flood losses in major coastal cities. Nat. Clim. Chang. 3 (9), 802–806.
Q. Zhou, G. Leng, and M. Huang, "Impacts of future climate change on urban flood risks: benefits of climate mitigation and adaptations," Hydrol. Earth Syst. Sci. Discuss., no. November, pp. 1–31, 2016.
Domingo, N., Refsgaard, A., Mark, O., Paludan, B., 2010. Flood analysis in mixed-urban areas reflecting interactions with the complete water cycle through coupled hydrologic-hydraulic modelling. Water Sci. Technol. 62 (6), 1386–1392.
Patro, S., Chatterjee, C., Mohanty, S., Singh, R., Raghuwanshi, N.S., 2009. Flood inundation modeling using MIKE FLOOD and remote sensing data. J. Indian Soc. Remote Sens. 37 (1), 107–118.
Sole, A., Giosa, L., Nolè, L., Medina, V., Bateman, A., 2008. Flood risk modelling with LiDAR technology. WIT Trans. Ecol. Environ. 118, 27–36.
Overton, I.C., 2005. Modelling floodplain inundation on a regulated river: Integrating GIS, remote sensing and hydrological models. River Res. Appl. 21 (9), 991–1001.
Muis, S., Güneralp, B., Jongman, B., Aerts, J.C.J.H., Ward, P.J., 2015. Flood risk and adaptation strategies under climate change and urban expansion: A probabilistic analysis using global data. Sci. Total Environ. 538, 445–457.
Tavares, A.O., dos Santos, P.P., Freire, P., Fortunato, A.B., Rilo, A., Sá, L., 2015. Flooding hazard in the Tagus estuarine area: The challenge of scale in vulnerability assessments. Environ. Sci. Policy 51, 238–255.
Garbutt, K., Ellul, C., Fujiyama, T., 2015. Mapping social vulnerability to flood hazard in Norfolk, England. Environ. Hazards 14 (2), 156–186.
Hunt, A., Watkiss, P., 2011. Climate change impacts and adaptation in cities: A review of the literature. Clim. Change 104 (1), 13–49.
L. Mucerino et al., "Coastal exposure assessment on Bonassola bay," Ocean Coast. Manag., vol. 167, no. May 2018, pp. 20–31, 2019.
Reid, A., Maratea, E., Kilaparty, B., Fang, T., 2014. "Final Floodplain Risk Management Study -. Alexandra Canal Floodplain Risk Management Study and Plan".
S. Shakrabarty, "Final Floodplain Risk Management Study - Marrickville Valley Floodplain Risk Management Study and Plan," 2017.
Rehan, B.M., 2018. An innovative micro-scale approach for vulnerability and flood risk assessment with the application to property-level protection adoptions. Nat. Hazards 91 (3), 1039–1057.
S. M. Tapsell, E. C. Penning-Rowsell, S. M. Tunstall, and T. L. Wilson, "Vulnerability to flooding : health," Philos. Trans. R. Soc. London, pp. 1511–1525, 2002.
Kammerbauer, M., Wamsler, C., 2018. Risikomanagement ohne Risikominderung? Soziale Verwundbarkeit im Wiederaufbau nach Hochwasser in DeutschlandRisk Management without Risk Reduction? The Role of Social Vulnerability in Post-Disaster Recovery after Floods in Germany. Raumforsch. und Raumordnung | Spat. Res. Plan. 76 (6), 485–496.
Connor, R.F., Hiroki, K., 2005. Development of a method for assessing flood vulnerability. Water Sci. Technol. 51 (5), 61–67.
S. F. Balica, N. G. Wright, and F. van der Meulen, A flood vulnerability index for coastal cities and its use in assessing climate change impacts, vol. 64, no. 1. 2012.
Yang, W., Xu, K., Lian, J., Ma, C., Bin, L., 2018. Integrated flood vulnerability assessment approach based on TOPSIS and Shannon entropy methods. Ecol. Ind. 89 (February), 269–280.
Szewrański, S., Świąder, M., Kazak, J.K., Tokarczyk-Dorociak, K., van Hoof, J., 2018. Socio-Environmental Vulnerability Mapping for Environmental and Flood Resilience Assessment: The Case of Ageing and Poverty in the City of Wrocław, Poland. Integr. Environ. Assess. Manag. 14 (5), 592–597.
J. S. Lee and H. Il Choi, "Comparison of flood vulnerability assessments to climate change by construction frameworks for a composite indicator," Sustain., vol. 10, no. 3, 2018.
Fernandez, P., Mourato, S., Moreira, M., Pereira, L., 2016. A new approach for computing a flood vulnerability index using cluster analysis. Phys. Chem. Earth. 94, 47–55.
Zachos, L.G., Swann, C.T., Altinakar, M.S., McGrath, M.Z., Thomas, D., 2016. Flood vulnerability indices and emergency management planning in the Yazoo Basin, Mississippi. Int. J. Disaster Risk Reduct. 18, 89–99.
Brouwer, R., Akter, S., Brander, L., Haque, E., 2007. Socioeconomic vulnerability and adaptation to environmental risk: A case study of climate change and flooding in Bangladesh. Risk Anal. 27 (2), 313–326.
Bhattacharjee, K., Behera, B., 2018. Determinants of household vulnerability and adaptation to floods: Empirical evidence from the Indian State of West Bengal. Int. J. Disaster Risk Reduct. 31 (July), 758–769.
Rana, I.A., Routray, J.K., 2018. Multidimensional Model for Vulnerability Assessment of Urban Flooding: An Empirical Study in Pakistan. Int. J. Disaster Risk Sci. 9 (3), 359–375.
Solín, M. Sládeková Madajová, and L. Michaleje, "Vulnerability assessment of households and its possible reflection in flood risk management: The case of the upper Myjava basin, Slovakia," Int. J. Disaster Risk Reduct., vol. 28, no. July 2017, pp. 640–652, 2018.
Queste, L., Lauwe, P., 2013. In: "User needs: Why we need indicators", in *Measuring Vulnerability to Natural Hazards. Towards Disaster Resilience Societies*. United Nations University Press, Bonn, pp. 103–115.
I. Török, "Qualitative assessment of social vulnerability to flood hazards in Romania," Sustain., vol. 10, no. 10, 2018.
Koks, E.E., Jongman, B., Husby, T.G., Botzen, W.J.W., 2015. Combining hazard, exposure and social vulnerability to provide lessons for flood risk management. Environ. Sci. Policy 47, 42–52.
Ford, J.D., Pearce, T., McDowell, G., Berrang-Ford, L., Sayles, J.S., Belfer, E., 2018. Vulnerability and its discontents: the past, present, and future of climate change vulnerability research. Clim. Change 151 (2), 189–203.
B. L. Turner et al., "A framework for vulnerability analysis in sustainability science," vol. 100, no. 14, 2003.
Rygel, L., O'Sullivan, D., Yarnal, B., 2006. A method for constructing a social vulnerability index: An application to hurricane storm surges in a developed country. Mitig. Adapt. Strateg. Glob. Chang. 11 (3), 741–764.
Van Manen, S.E., Brinkhuis, M., 2005. Quantitative flood risk assessment for Polders. Reliab. Eng. Syst. Saf. 90 (2–3), 229–237.
Cutter, S.L., Emrich, C.T., Morath, D.P., Dunning, C.M., 2013. Integrating social vulnerability into federal flood risk management planning. J. Flood Risk Manag. 6 (4), 332–344.
Sarewitz, D., Pielke, R., Keykhah, M., 2003. Vulnerability and risk: Some thoughts from a political and policy perspective. Risk Anal. 23 (4), 805–810.
Solangaarachchi, D., Griffin, A.L., Doherty, M.D., 2012. Social vulnerability in the context of bushfire risk at the urban-bush interface in Sydney: A case study of the Blue Mountains and Ku-ring-gai local council areas. Nat. Hazards 64 (2), 1873–1898.
Zahran, S., Brody, S.D., Peacock, W.G., Vedlitz, A., Grover, H., 2008. Social vulnerability and the natural and built environment: A model of flood casualties in Texas. Disasters 32 (4), 537–560.
Cutter, S.L., Boruff, B.J., Shirley, W.L., 2003. "Social Vulnerability to Environmental Hazards Social Vulnerability to. Environmental" 84 (2), 242–261.
O'Brien, P.W., Mileti, D.S., 1993. Citizen participation in emergency response. U.S. Geol. Surv. Prof. Pap. vol. 1553 B, 23–30.
Cutter, S.L., Mitchell, J.T., Scott, M.S., 2000. Revealing the vulnerability of people and places: A case study of georgetown county, South Carolina. Ann. Assoc. Am. Geogr. 90 (4), 713–737.
Blaikie, P., Cannon, T., Davis, I., Wisner, B., 2014. *At Risk: Natural Hazards, People's Vulnerability and Disasters*, 2nd editio. Routledge, London.
a. Fekete, "Validation of a social vulnerability index in context to river-floods in Germany," Nat. Hazards Earth Syst. Sci., vol. 9, no. 2, pp. 393–403, 2009.
Morrow, B.H., 1999. Identifying and mapping community vulnerability. Disasters 23 (1), 1–18.
Watts, B., Vale, D., Mulgan, G., Dale, M., Ali, R., Norman, W., 2009. "Sinking & Swimming. Understanding Britain's Unmet Needs", London.
Pulido, L., 2000. Rethinking environmental racism: White privilege and urban development in southern California. Ann. Assoc. Am. Geogr. 90 (1), 12–40.
K. A. Borden, M. C. Schmidtlein, C. T. Emrich, W. W. Piegorsch, and S. L. Cutter, "Vulnerability of U.S. cities to environmental hazards," J. Homel. Secur. Emerg. Manag., vol. 4, no. 2, 2007.
Holand, I.S., Lujala, P., Rod, J.K., 2011. Social vulnerability assessment for Norway: A quantitative approach. Nor. Geogr. Tidsskr. 65 (1), 1–17.
A. Dwyer, C. Zoppou, O. Nielsen, S. Day, and S. Roberts, "Quantifying Social Vulnerability : A methodology for identifying those at risk to natural hazards," Geosci. Aust., p. 101, 2004.

Apotsos, A., 2019. Mapping relative social vulnerability in six mostly urban municipalities in South Africa. Appl. Geogr. 105 (February), 86–101.
Kirby, R.H., Reams, M.A., Lam, N.S.N., Zou, L., Dekker, G.G.J., Fundter, D.Q.P., 2019. Assessing social vulnerability to flood hazards in the Dutch Province of Zeeland. Int. J. Disaster Risk Sci. 10 (2), 233–243.
K. Vincent, "Creating an index of social vulnerability to climate change for Africa," Tyndall Cent. Clim. Chang. Res., vol. 56, no. August, p. 41, 2004.
Schmidtlein, M.C., Deutsch, R.C., Piegorsch, W.W., Cutter, S.L., 2008. A sensitivity analysis of the social vulnerability index. Risk Anal. 28 (4), 1099–1114.
Frigerio, I., De Amicis, M., 2016. Mapping social vulnerability to natural hazards in Italy: A suitable tool for risk mitigation strategies. Environ. Sci. Policy 63, 187–196.
F. Fatemi, A. Ardalan, B. Aguirre, N. Mansouri, and I. Mohammadfam, "Social vulnerability indicators in disasters: Findings from a systematic review," Int. J. Disaster Risk Reduct., vol. 22, no. June 2016, pp. 219–227, 2017.
Tonmoy, F.N., El-Zein, A., Hinkel, J., 2014. Assessment of vulnerability to climate change using indicators: A meta-analysis of the literature. Wiley Interdiscip. Rev. Clim. Chang. 5 (6), 775–792.
El-Zein, A., Tonmoy, F.N., 2017. Nonlinearity, fuzziness and incommensurability in indicator-based assessments of vulnerability to climate change: A new mathematical framework. Ecol. Ind. 82 (March), 82–93.
Rufat, S., Tate, E., Burton, C.G., Maroof, A.S., 2015. Social vulnerability to floods: Review of case studies and implications for measurement. Int. J. Disaster Risk Reduct. 14, 470–486.
Ebert, U., Welsch, H., 2004. Meaningful environmental indices: A social choice approach. J. Environ. Econ. Manage. 47 (2), 270–283.
El-Zein, A., Tonmoy, F.N., 2015. Assessment of vulnerability to climate change using a multi-criteria outranking approach with application to heat stress in Sydney. Ecol. Ind. 48, 207–217.
Crichton, D., 2002. UK and Global Insurance Responses to Flood Hazard. Water Int. 27 (1), 119–131.
Lindley, S.J., Handley, J.F., Theuray, N., Peet, E., Mcevoy, D., 2006. Adaptation strategies for climate change in the urban environment: Assessing climate change related risk in UK urban areas. J. Risk Res. 9 (5), 543–568.
Dang, N.M., Babel, M.S., Luong, H.T., 2011. Evaluation of food risk parameters in the Day River Flood Diversion Area, Red River Delta, Vietnam. Nat. Hazards 56 (1), 169–194.
Kaźmierczak, A., Cavan, G., 2011. Surface water flooding risk to urban communities: Analysis of vulnerability, hazard and exposure. Landsc. Urban Plan. 103 (2), 185–197.
Plate, E.J., 2002. Flood risk and flood management. J. Hydrol. 267 (1–2), 2–11.
Schanze, J., 2006. In: "NoFlood risk management – a basic framework", in *Flood Risk Management: Hazards, Vulnerability and Mitigation Measures*. Springer, pp. 1–20.
B. L. Mckenny, J. Saulwick, and J. Tovey, "After the flood : Sydney counts the cost of record rains," Sydney Morning Herald, Sydney, pp. 1–3, 09-Mar-2019.
O'Loughlin, G., Stack, B., Kus, B., 2018. "DRAINS User Manual".
Ball, I., 2016. J; Babister, M; Nathan, R; Weeks, W; Weinmann, PE; Retallick, M; Testoni. A Guide to Flood Estimation, Australian Rainfall and Runoff.
CSIRO and Bureau of Meteorology, Climate Change in Australia Projections for Australia's Natural Resource Management Regions: Technical Report. 2015.
Jean Palutikof; David Rissik; Steven Webb; Fahim Tonmoy; Sarah Boulter; Anne Leitch; Ana Perez Vidaurre; Kim Wilson; Marilee Campbell., "CoastAdapt: A changing climate in coastal Australia: Build knowledge, take action," 2017. [Online]. Available: https://coastadapt.com.au/. [Accessed: 30-Dec-2019].
New South Wales Government, "Floodplain Development Manual - The Mnaagement of Flood Liable Land," Sydney, 2005.
Geoscience Australia, "National Exposure Information System (NEXIS)," 2019. [Online]. Available: https://www.ga.gov.au/scientific-topics/community-safety/risk-and-impact/nexis. [Accessed: 30-Dec-2019].
Field, A., 2009. Discovering Statistic using SPSS (and sex and drugs and rock "n" roll), 2nd ed. SAGE, London.
Kaiser, H.F., 1970. A Second Generation Little Jiffy. Psychometrika 35 (4), 401–415.
H. F. Kaiser, "The Application of Electronic Computers to Factor Analysis," Educ. Psychol. Meas., vol. XX, no. 1, pp. 141–151, 1960.
B. Pink, "Socio-Economic Indexes for Areas (SEIFA) 2011 - Technical Paper.," Canberra, 2013.
Ahmed, T., 2018. Vulnerability to Flooding in Cities at Local Scale : New Methodology with Application to a Local Council in Sydney. University of Sydney.
S. A. Levin and S. A. Levin, "The problem of pattern and scale in ecology," vol. 73, no. August 1989, pp. 1943–1967, 1992.
M. Convertino and L. J. J. Valverde, "Toward a pluralistic conception of resilience," Ecol. Indic., vol. 107, no. June, p. 105510, 2019.
Willems, P., Arnbjerg-Nielsen, K., Olsson, J., Nguyen, V.T.V., 2012. Climate change impact assessment on urban rainfall extremes and urban drainage: Methods and shortcomings. Atmos. Res. 103, 106–118.
Loaiciga, H.A., Valdes, J.B., Vogel, R., Garvey, J., Schwarz, H., 1996. Global warming and the hydrologic cycle. J. Hydrol. 174 (1–2), 83–127.
Adger, W.N., 2000. Social and ecological resilience: Are they related? Prog. Hum. Geogr. 24 (3), 347–364.
Berkes, F., Folke, C., Colding, J., 1998. Linking Social and Ecological Systems: Management Practices and Social Mechanisms for Building Resilience. Cambridge University Press.
Satterthwaite, D., 2003. The Links between Poverty and the Environment in Urban Areas of Africa, Asia, and Latin America. Ann. Am. Acad. Pol. Soc. Sci. 590, 73–92.
Fielding, J., Burningham, K., 2005. Environmental inequality and flood hazard. Local Environ. 10 (4), 379–395.
Schreider, S.Y., Smith, D.I., Jakeman, A.J., 2000. Climate change impacts on urban flooding. Clim. Change 47 (1–2), 91–115.
Ashley, R.M., Balmfort, D.J., Saul, A.J., Blanskby, J.D., 2005. Flooding in the future - Predicting climate change, risks and responses in urban areas. Water Sci. Technol. 52 (5), 265–273.
Berggren, K., Olofsson, M., Viklander, M., Svensson, G., Gustafsson, A.M., 2011. Hydraulic Impacts on Urban Drainage Systems due to Changes in Rainfall Caused by Climatic Change. J. Hydrol. Eng. 17 (1), 92–98.
Zhu, T., Lund, J.R., Jenkins, M.W., Marques, G.F., Ritzema, R.S., 2007. Climate change, urbanization, and optimal long-term floodplain protection. Water Resour. Res. 43 (6), 1–11.
H. Chang, M. Lafrenz, I.-W. Jung, M. Figliozzi, and D. Platman, "Potential Impacts of Climate Change on Urban Flooding: Implications for Transportation Infrastructure and Travel Disruption," in International Conference on Ecology and Transportation (ICOET) 2009, 2010, p. pp 72-79.
Ahmed, F., Moors, E., Khan, M.S.A., Warner, J., Terwisscha van Scheltinga, C., 2018. Tipping points in adaptation to urban flooding under climate change and urban growth: The case of the Dhaka megacity. Land use policy 79 (May), 496–506.
Kelman, I., Spence, R., 2004. An overview of flood actions on buildings. Eng. Geol. 73 (3–4), 297–309.
Soetanto, R., Proverbs, D.G., 2004. Impact of flood characteristics on damage caused to UK domestic properties: the perceptions of building surveyors. Struct. Surv. 22 (2), 95–104.
Ezer, T., Atkinson, L.P., 2014. Accelerated flooding along the U.S. East Coast: On the impact of sea-level rise, tides, storms, the Gulf Stream, and the North Atlantic Oscillations. Earth's Futur. 2 (8), 362–382.
Adger, W.N., Aug. 2006. Vulnerability. Glob. Environ. Chang. 16 (3), 268–281.
A. M. Wellstead, M. Howlett, and J. Rayner, "The neglect of governance in forest sector vulnerability assessments: Structural-functionalism and 'Black Box' problems in climate change adaptation planning," Ecol. Soc., vol. 18, no. 3, 2013.
Wise, R.M., et al., 2014. Reconceptualising adaptation to climate change as part of pathways of change and response. Glob. Environ. Chang. 28, 325–336.
T. Wolf, W. Chuang, and G. Mcgregor, "On the Science-Policy Bridge : Do Spatial Heat Vulnerability Assessment Studies Influence Policy ?," pp. 13321–13349, 2015.
Saltelli, A., Tarantola, S., Campolongo, F., Ratto, M., 2004. Sensitivity Analysis in Practice: a Guide to Assessing Scientific Models. Wiley, Chichester.
M. Convertino, A. Annis, and F. Nardi, "Information-theoretic portfolio decision model for optimal flood management," Environ. Model. Softw., vol. 119, no. December 2018, pp. 258–274, 2019.